BMC Microbiology

RESEARCH Open Access

Wolbachia elevates host methyltransferase expression and alters the m^{6}A methylation landscape in *Aedes aegypti* mosquito cells

Michael Leitner[1], Valentine Murigneux[2], Kayvan Etebari[3] and Sassan Asgari[1*]

Abstract

Wolbachia pipientis is an intracellular endosymbiotic bacterium that blocks the replication of several arboviruses in transinfected *Aedes aegypti* mosquitoes, yet its antiviral mechanism remains unknown. For the first time, we employed Nanopore direct RNA sequencing technology to investigate the impact of *w*AlbB strain of *Wolbachia* on the host's N^6-methyladenosine (m^{6}A) machinery and post-transcriptional modification landscape. Our study revealed that *Wolbachia* infection elevates the expression of genes involved in the mosquito's m^{6}A methyltransferase complex. However, knocking down these m^{6}A-related genes did not affect *Wolbachia* density. Nanopore sequencing identified 1,392 differentially modified m^{6}A DRACH motifs on mosquito transcripts, with 776 showing increased and 616 showing decreased m^{6}A levels due to *Wolbachia*. These m^{6}A sites were predominantly enriched in coding sequences and 3′-untranslated regions. Gene Ontology analysis revealed that genes with reduced m^{6}A levels were over-represented in functional GO terms associated with purine nucleotide binding functions critical in the post-transcriptional modification process of m^{6}A. Differential gene expression analysis of the Nanopore data uncovered that a total of 643 protein-coding genes were significantly differentially expressed, 427 were downregulated, and 216 were upregulated. Several classical and non-classical immune-related genes were amongst the downregulated DEGs. Notably, it revealed a critical host factor, transmembrane protein 41B (TMEM41B), which is required for flavivirus infection, was upregulated and methylated in the presence of *Wolbachia*. Indeed, there is a strong correlation between gene expression being upregulated in genes with both increased and decreased levels of m^{6}A modification, respectively. Our findings underscore *Wolbachia*'s ability to modulate many intracellular aspects of its mosquito host by influencing post-transcriptional m^{6}A modifications and gene expression, and it unveils a potential link behind its antiviral properties.

Keywords *Aedes aegypti*, *w*AlbB, *Wolbachia*, m^{6}A, Post-transcriptional modification, TMEM41B, Flavivirus host factor, Gene expression, Mosquito

*Correspondence:
Sassan Asgari
s.asgari@uq.edu.au
[1]School of the Environment, The University of Queensland, Brisbane, Australia
[2]QCIF Facility for Advanced Bioinformatics, Institute for Molecular Bioscience, The University of Queensland, Brisbane, Australia
[3]School of Agriculture and Food Sustainability, The University of Queensland, Brisbane, Australia

Introduction

Mosquito-borne flaviviruses represent a significant risk to public health. *Aedes aegypti* is the primary vector that transmits several pathogenic arthropod-borne viruses (arbovirus) such as dengue, Zika, Chikungunya, and yellow fever viruses [62, 76, 104]. In the absence of effective vaccines or anti-viral drugs and the inefficiency of chemical-based control measures, viable transmission control alternatives are being investigated to reduce the spread of arboviruses. One successful approach uses the endosymbiotic bacterium *Wolbachia pipientis* in transinfected mosquitoes to suppress virus replication and transmission of arboviruses [7, 15, 21, 42, 49, 87, 91, 113]. However, the *Wolbachia*-mediated antiviral mechanism remains poorly understood. Despite considerable efforts, none of the proposed individual mechanisms fully explain the virus-blocking phenotype.

Previous studies predominantly associated *Wolbachia*'s contribution to the virus blocking phenotype in insects to either induction of the immune system [6, 15, 55, 97, 103, 117, 137, 140], competition for essential cellular host resources and space [19, 34, 52, 90, 117, 129], inhibition of viral entry [81], and modulation of various pro- and anti-viral genes [9, 31, 40, 46, 60, 81, 139]. Further, the density of *Wolbachia* within host cells and tissues was found to determine the strength of *Wolbachia*'s virus blocking phenotype [22, 80, 85]. However, more recent research indicated that the extent of *Wolbachia*-mediated blocking of arboviruses is neither *Wolbachia* density-dependent nor tissue-specific in *Ae. aegypti* [4, 21, 32].

The degree of viral inhibition differs significantly among *Wolbachia* strains, with some showing no inhibition, while others achieve substantial blocking [7, 22, 85, 86]. The strains *w*MelPop and *w*Au reach very high densities and exhibit strong transmission blocking [7, 84, 91]. However, high *Wolbachia* densities are also linked to increased virulence in the host, adversely impacting various life-history traits such as reproductive fitness, lifespan, and egg survival [7, 88, 95, 106]. Conversely, the *Wolbachia* strain *w*AlbB, maintains moderate density levels in *Ae. aegypti* and has only mild negative effects on host fitness, yet it still provides strong virus transmission inhibition [1, 7, 10, 15, 54, 83].

These admirable characteristics are likely a result of a complex web of molecular interactions between the symbiont and host. Recent studies have shown that *Wolbachia*-mediated virus inhibition occurs at early stages post-infection in *Drosophila* and mosquito cells [11, 12, 47, 102]. These suggested that viral RNA is the target, which encounters rapid degradation upon virus entry [11, 12, 47, 102]. In our recent study, genes encoding cytosine (m^5C) and N^6-adenosine methyltransferases (m^6A) and SUMOylation pathway, involved in post-transcriptional modifications were elevated at the early hours of DENV infection in *Wolbachia*-transinfected *Ae. aegypti* mosquito cells [65].

Post-transcriptional modifications are key regulators of biological processes across eukaryotes, and more than 100 different chemical RNA modifications have been characterised [17, 18]. However, methylation at the N^6-position of adenosine (m^6A) is the most abundant modification found on RNA of cellular, coding, non-coding, and possibly viral RNAs [17, 24, 36]. It has been established that m^6A RNA modifications regulate many essential cellular processes such as gene expression, RNA splicing, mRNA stability, translation, microRNA biogenesis, and host-virus interactions [2, 33, 35–37, 48, 131]. There are three main protein groups involved in the dynamic and reversible regulation of m^6A modifications: methyltransferases (m^6A-writers), demethylases (m^6A-erasers), and m^6A binding proteins (m^6A-readers) [48, 73]. m^6A is added to mRNA by the core complex of methyltransferase-like protein 3 (METTL3) and METTL14 [73]. METTL3 is the catalytic subunit, METTL14 is an essential component that features RNA binding properties, and WTAP is a stabilising factor [73, 125]. The METTL3-METTL14-WTAP complex targets the consensus motif DRACH (where D = G/A/U, R = G/A and H = U/A/C) in mRNAs [23, 33, 58]. The methylation can be removed by m^6A-erasers such as obesity-associated protein (FTO) and AlkB homolog 5 (ALKBH5) [48, 51, 142]. Lastly, m^6A-readers bind specifically to m^6A-modified RNAs and modulate protein-RNA interactions or subsequent regulatory functions such as stability, localisation, alternative splicing, degradation, and translation of m^6A-modified mRNA [8, 56, 74, 75, 126, 133]. The main readers for m^6A methylation in the nucleus are heterogeneous nuclear ribonucleoprotein C family members (HNRNPC) and HNRNPA2B1, and in the cytoplasm, the YT521-B homology (YTH) domain-containing proteins (YTHDF1-3 and YTHDC1–2) [2, 48, 64, 74, 75, 111].

The present knowledge in this relatively unexplored field of research is limited to human cells and *Drosophila melanogaster* [35, 36, 109]. Gokhale et al. [36] demonstrated the presence of m^6A modification on flavivirus RNA and their role in regulating the life cycle of viruses. The study by Shah et al. [109] identified m^6A RNA modifications in *Drosophila* adult females to be highly enriched in genes associated with developmental, regulatory, and neuronal functions, and their expression was considerably more tissue-specific than unmethylated genes. They only assessed the m^6A-positions across the *D. melanogaster* genome using two biological replicates without *Wolbachia* and virus infection. More recent studies identified the presence of m^6A modifications on the mRNA from *Ae. aegypti* Aag2 cell line and mosquito species *Anopheles sinensis* [26, 71]. These studies further

reported that m^6A methylation modulated viral infection and sperm tail formation.

Wolbachia also has recently been implicated in differential viral RNA modifications in mosquito cells [14]. They found evidence of altered C5 cytosine methyltransferase (DNMT2), m^6A expression, and viral RNA methylation in mosquito cells in the presence of *Wolbachia* and Sindbis virus [14]. In consideration of these recent and novel observations of altered post-transcriptional modifications in the presence of *Wolbachia*, we investigated differences in m^6A expression levels and altered post-transcriptional modifications in the presence and the absence of *Wolbachia* in Aag2 and Aag2.*w*AlbB cells using Nanopore technology. Our results show that m^6A gene machinery expression was elevated, and the number of differentially modified m^6A sites on host mRNA transcripts significantly increased in *Wolbachia*-transinfected cells. We also determined differentially expressed genes due to *Wolbachia* infection for the first time with Nanopore sequencing. Understanding m^6A modifications in the mosquito vector *Ae. aegypti*, its role in the biology of the mosquito, and whether the m^6A landscape is altered in the presence of *Wolbachia* will provide new insights into the intrinsic mosquito-*Wolbachia* interaction.

Methods

Mosquito cell line

Aedes aegypti (Aag2)-embryonic-derived cell line persistently infected with *w*AlbB strain of *Wolbachia* (Aag2.*w* AlbB) [16], *w*MelPop-infected Aag2 cells (Aag2.*w*MelPop) [46], and uninfected Aag2 cells were maintained as cell monolayers in flask in a 1:1 mixture of Mitsuhashi–Maramorosch and Schneider's Insect Medium (Invitrogen), supplemented with 10% fetal bovine serum (FBS) at 27 °C.

Reverse transcription quantitative PCR (RT-qPCR)

Total RNA was extracted from cells using Qiazol according to the manufacturer's instructions (Qiagen). RNA was then treated with Turbo DNase (Invitrogen) and reverse transcribed using M-MuLV reverse transcriptase (New England Biolabs) with oligo (dT) primer according to the manufacturer's instructions. No-reverse transcriptase and positive control reactions were also included in the reverse transcription-PCR (RT-PCR). The synthesized cDNAs were diluted in a 1:10 ratio with Ultrapure DNase/RNase-free water (Invitrogen) and used in RT-qPCR reactions. All reactions were carried out using the QuantiFast SYBR Green PCR Kit (Qiagen) and a Rotor-Gene Q thermocycler (Qiagen) as per the manufacturer's instructions. *Ae. aegypti*'s *ribosomal protein S17* (*RPS17*) gene was used as the normalizing gene [91]. The relative expression of target genes and *RPS17* was measured using the relative quantification method as described previously [100]. The gene expression levels in controls were adjusted to 1, and the transcript levels in treatments are expressed relative to the controls. All primers used in this study are listed in Table S1.

Genomic DNA extraction and determination of *Wolbachia* density

Genomic DNA was extracted from *Wolbachia* cells with EconoSpin silica membrane columns (Epoch Life Science) using a previously described protocol [105]. The relative densities of *w*AlbB and *w*MelPop cells were determined by qPCR, using specific primers for the relevant strain's *Wolbachia surface protein* gene (*wsp*) and *Ae. aegypti*'s *RPS17* as the normalizing gene [91].

Knocking down m^6A machinery genes

The potential effect of knocking down m^6A machinery genes on *Wolbachia* density in Aag2.*w*AlbB cells was evaluated by RNA interference (RNAi)-mediated gene silencing. For each gene, primers were designed that contained T7 promotor sequences in both forward and reverse primers. MEGAscript T7 transcription kit (Invitrogen) was used to generate dsRNA (~500 bp in size) from the amplified PCR fragment as per the manufacturer's instructions. The dsRNA products for each of the m^6A genes were cloned into the pGEM-T Easy vector (Promega) and confirmed by Sanger sequencing. Aag2.*w*AlbB cells were transfected with Cellfectin II reagent (Invitrogen) and serum-free transfection medium. Transfection was performed in 12-well plates in replicates, including Cellfectin II (Invitrogen) and serum-free transfection medium-only treated cells, dsGFP as a negative control, and about 2 µg of dsRNA specific to the m^6A genes. Cells were incubated for 3 h at 27°C followed by adding cell culture medium containing 2% FBS and incubating for a further 48 h. A second transfection was performed two days after the first one, and cells were collected for total RNA extraction, as described above. Total RNA and DNA were extracted, reverse transcribed (for RNA), and analysed by RT-qPCR and qPCR to evaluate gene silencing and *Wolbachia* density, respectively.

Nanopore direct RNA sequencing

To investigate the m^6A methylation status at single-nucleotide resolution in mRNA, Aag2.*w*AlbB and *Wolbachia*-free Aag2 cells in three replicates for each experimental condition were used to examine differences in the presence or absence of *Wolbachia*. Prior to the experiment, *w*AlbB's density was quantified by qPCR as described above. Total RNA was extracted using the RNeasy mini extraction kit (Qiagen) according to the manufacturer's instructions, and RNA concentration and purity were measured by spectrophotometry (Epoch, BioTek).

The purification of mRNA from total RNA by Dynabeads mRNA purification kit (Invitrogen), direct RNA-Seq library preparation, and Oxford Nanopore sequencing utilizing the PromethION flow cell technology was performed by the Garvan Institute of Medical Research in New South Wales. Nanopore direct RNA sequencing (DRS) included the use of R9.4.1 flow cells (FLO-PRO002) and direct RNA-Seq kit (SQK-RNA002). Data acquisition and basecalling were performed by using Oxford Nanopore MinKNOW software (v.22.03.4) and its integrated basecalling algorithm Guppy (v.6.0.7 + c7819bc52) in high accuracy model (rna_r9.4.1_70bps_hac_prom) configuration. Only reads with a quality score above 7 (min_qscore = 7) were selected. Sequencing data were acquired as raw signal (FAST5/SLOW5) and basecalled (FASTQ) files. The read basecalling, mapping metrics, and RNA sample quality and yield are listed in Tables S2.

Preprocessing of reads and alignment to transcriptome

The basecalled FASTQ reads were aligned to the *Ae. aegypti* LVP_AGWG AaegL5.3 reference transcriptome downloaded from (https://vectorbase.org/vectorbase/app/) using minimap2 (v.2.24-r1122) with the settings (minimap2 -ax map-ont -uf -t 6 --secondary = no) and a concatenated FASTA file containing coding and noncoding RNA reference annotations https://vectorbase.org/common/downloads/Current_Release/AaegyptiLVP_AGWG/fasta/data/) [67, 68]. The resulting sequence alignment map (SAM) files were converted to binary alignment map (BAM) files and all reads were sorted and indexed using SAMtools (v.1.9) [27, 69]. Nanopolish (v.0.14.0) was used to realign/resquiggle the raw signal SLOW5 reads and basecalled FASTQ reads to the expected reference sequence with settings (nanopolish index --slow5 nanopolish eventalign --reads --bam --genome --signal-index --scale-events --summary --threads 16) [77]. Nanopolish is freely available on github under the open-source MIT license (https://github.com/jts/nanopolish).

m^{6}A methylation analysis

The evaluation of m^{6}A methylation in a 5-kmer was performed with xPore (v.2.1), a Python package for the identification of differential RNA modifications from Nanopore sequencing data [101]. Specifically, xpore-dataprep (xpore dataprep --eventalign --out_dir) and xpore-diffmod (xpore diffmod --config --n_processes 16) command line to process the segmented raw signal file and model differential modifications were used as per the instructions [101]. xPore applies a multi-sample two-Gaussian mixture distribution model followed by a two-tailed, unpooled z-test on the modification-rate difference of any two conditions for each position. The resulting p values were adjusted for multiple comparisons using the Benjamini–Hochberg correction.

Genomic alignment for gene expression analysis

The basecalled FASTQ reads were aligned to the *Ae. aegypti* LVP_AGWG AaegL5.3 genomic reference FASTA file using minimap2 (v.2.24) with the settings (minimap2 -ax splice -uf -k14) accounting for splicing [67, 68]. Generated SAM files were converted to BAM files using SAMtools (v.1.13) [27, 69].

Transcript quantification

Bambu (v.3.2.4) multiple samples settings (se.multiSample <- bambu(reads = c(WB_1, WB_2, WB_3, Aag2_1, Aag2_2, Aag2_3), annotations = gtf, genome = fasta)) including genomic alignment sample BAM files, *Ae. aegypti* LVP_AGWG AaegL5.3 nucleotide sequences genomic reference FASTA file, and GTF annotation file were used as per the instructions for transcript quantification [20]. Bambu is an R package available on github under the GNU general public version 3.0 license (https://github.com/GoekeLab/bambu).

Differential gene expression analysis with DESeq2

Quantified transcript file (se.multiSample) was loaded in DESeq2 (v. 1.40.1) and developers' instructions were followed for the analysis of differentially expressed genes [79]. DESeq2 is an R package available on bioconductor under the GNU lesser general public license (https://bioconductor.org/packages/devel/bioc/vignettes/DESeq2/inst/doc/DESeq2.html).

For data visualisation and generation of graphs, ggplot2 was used as per the instructions. ggplot2 is an open-source data visualization R package available on tidyverse under the MIT license (https://ggplot2.tidyverse.org/LICENSE.html). The threshold of statistical significance for identified DEG's was set to false discovery rate (FDR) of less than 0.05 and $\log_2$ fold change greater than 2.

Differential gene expression analysis with CLC genomics workbench

The RNA-Seq analysis for long reads (beta v. 1.1) with long read support (v.22.0.1) and incorporated minimap2 was used to align the basecalled FASTQ reads to the *Ae. aegypti* LVP_AGWG AaegL5.3 with default settings [68]. Principal component analysis (PCA) graphs were produced between *Wolbachia*-transinfected Aag2.*w*AlbB and *Wolbachia*-free Aag2 cells that served as a control to identify any outlying samples within the dataset. The CLC-GWB differential expression for RNA-Seq tool with the default parameters was used to identify DEGs between Aag2.*w*AlbB and Aag2 samples. The relative expression levels were produced as RPKM (reads per kilobase of transcript per million reads mapped) values,

which accounts for the relative size of the transcripts normalising for sequencing depth.

Validation of DEGs using quantitative reverse transcription-PCR

For validation of the differentially expressed *Ae. aegypti* genes identified through differential gene analysis using DESeq2 and CLC, a total of nine up- and downregulated genes were selected. The NCBI Primer-BLAST primer design tool was used to design primers for the selected DEGs and the *Ae. aegypti RPS17* gene was used as the normalizing gene [91, 135]. All primers used in this study are listed in Table S1. RNA samples from Aag2 and Aag2.*w*AlbB previously extracted for the gene expression analysis were used for validating the differentially expressed mosquito genes. Reverse transcription, and qPCR were performed as described above. The relative abundance of *Ae. aegypti RPS17* gene and selected DEGs were determined using the relative quantification method as described previously [100].

Knocking down *TMEM41B* and virus infection

To evaluate the potential effect of knocking down *TMEM41B* on virus replication, Aag2 cells were seeded into a 12-well culture plate (Greiner Bio-One) at 1.5×10^6 cells per well and allowed to adhere for 1 h at 27 °C. Cells were transinfected with Cellfectin II reagent (Invitrogen) and serum-free transfection medium. Transfection was performed in 12-well plates in replicates, including Cellfectin II (Invitrogen) and serum-free transfection medium-only treated cells, dsGFP as a negative control, and about 2 µg of dsRNA specific to the *TMEM41B* gene. Cells were incubated for 3 h at 27°C followed by adding cell culture medium containing 2% FBS and incubating for a further 48 h. A second transfection was performed two days after the first one, the medium was then removed, and cells were inoculated with DENV serotype 2 (DENV-2) East Timor strain (ET-300) at a multiplicity of infection (MOI) of 1. The 12-well plate was incubated on a rocker for 1 h at room temperature followed by the removal of supernatant and subsequent replenishment with fresh medium containing 2% FBS. The plate was then incubated for 48 h at 27 °C, and cells were collected for total RNA extraction, as described above. Total RNA was extracted, reverse transcribed, and analysed by RT-qPCR with both forward and reverse gene-specific primers (DENV2-qF and DENV2-qR) (Table S1) used to amplify the DENV-2 NS5 region of the viral genome [9]. *Ae. aegypti RPS17* forward and reverse primers were used to amplify the normalizing gene [91]. All qPCRs were performed in duplicates using a Rotor-Gene Q thermocycler (Qiagen) under the conditions specified above.

Gene ontology analysis

Differentially expressed *Ae. aegypti* genes identified by CLC-GWB were submitted to Blast2GO for gene ontology (GO) [38]. We used Basic Local Alignment Search Tool (BLAST) and InterProScan algorithms to identify GO terms of DEGs [53]. Enrichment analysis using Fisher's exact test of down- and upregulated DEGs was performed to find over- and under-represented terms for each category of molecular function, biological process, and cellular components [3]. GO terms were considered significantly enriched with a p value of 0.05 adjusted for multiple comparisons using the Benjamini–Hochberg (FDR) correction. The identical Blast2GO for GO term analysis settings were used for genes containing differentially modified m^{6}A DRACH motifs.

Results

Expression of m^{6}A genes in the presence and absence of *Wolbachia*

Prior to assessing the expression of the m^{6}A genes, the density of *Wolbachia* was examined in cell lines. The average density expressed in standard error of the mean (± SEM) of *w*AlbB *Wolbachia* passage 10–11, and Aag2.*w*MelPop passage 30–31 used in the in vitro m^{6}A gene expression experiments was at about comparable densities of *Wolbachia* at 145, 107, and 136, 111 per cell, respectively (Fig. 1A and B).

The initial results showed that m^{6}A-writer methyltransferase-like 3 (METTL3) was significantly upregulated (One-way ANOVA, $p < 0.0001$) in the presence of *w*AlbB strain of *Wolbachia* compared to *Wolbachia*-free cells. In contrast, no significant difference in the expression levels for m^{6}A-writer *AeMETTL3* in the *w*MelPop strain of *Wolbachia* was observed between the infected and uninfected cells (Fig. 2A). The expression of the m^{6}A-writer methyltransferase-like 14 (METTL14) was also only upregulated (One-way ANOVA, $p < 0.0164$) in the presence of the *w*AlbB strain of *Wolbachia* compared to *Wolbachia*-free cells. No significant difference in the expression levels for m^{6}A-writer *AeMETTL14* in the *w*MelPop strain of *Wolbachia* was evident between the infected and uninfected cells (Fig. 2B). However, this was different for the m^{6}A-reader *AeYTHDF3* encoding gene, which was upregulated in the presence of both *w*AlbB (One-way ANOVA, $p < 0.0001$) and *w*MelPop (Dunnet *post-hoc* test $p < 0.0249$) strains of *Wolbachia* compared to *Wolbachia*-free cells (Fig. 2C). Expression of the m^{6}A-eraser *AeALKBH8* encoding gene [25] was also slightly upregulated (One-way ANOVA, $p < 0.0175$) in the presence of the *w*AlbB strain of *Wolbachia* compared to *Wolbachia*-free cells. Still no significant difference in the expression levels was observed in the presence of the *w*MelPop strain of *Wolbachia* between the infected and uninfected cells (Fig. 2D).

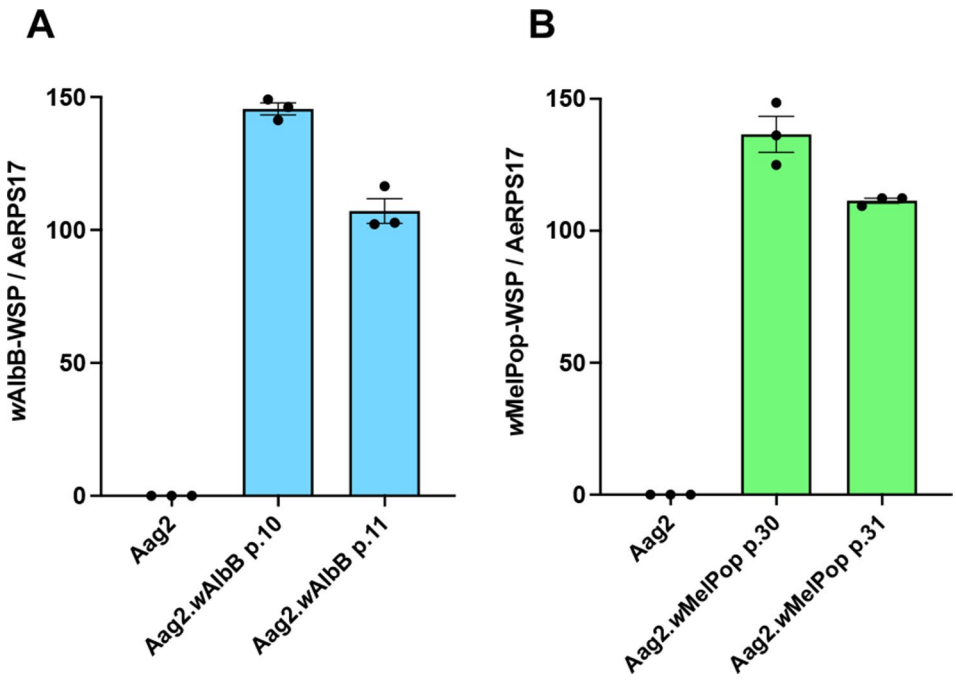

Fig. 1 Relative density of *Wolbachia* in Aag2.*w*AlbB (**A**) and Aag2.*w*MelPop (**B**) cell lines. The relative density of *Wolbachia* was determined by qPCR analysis using genomic DNA extracted from Aag2.*w*AlbB, Aag2.*w*MelPop, and *Wolbachia*-free Aag2 cells that served as a control. The numbers on each dataset show the average *Wolbachia* density of the three biological replicates in each cell line. Density is expressed as the mean ratio between the *Wolbachia* surface protein gene (*wsp*) and *Ae. aegyptiPRS17* was used as the normalizing gene. The error bars represent the standard error of the mean (SEM) of the three biological replicates

Double-stranded RNA-mediated knockdown of m^{6}A-writers, -reader, and -eraser does not affect *Wolbachia* density

To find out whether knocking down m^{6}A modification genes has any effect on *Wolbachia* density in Aag2.*w*AlbB cells, we used dsRNA specific to *Ae. aegypti* m^{6}A-writers, -reader, and -eraser. Cells were transfected with m^{6}A-gene-specific or non-targeting dsRNA (dsGFP). Following RNA extraction from harvested cells, RT-qPCR quantification of m^{6}A-writers, -reader, and -eraser gene expression showed an average knockdown of 82% (Fig. 3A), 75% (Fig. 3B), 61% (Fig. 4A), and 63% (Fig. 4B) relative to non-targeting GFP controls. However, *Wolbachia* density was not affected (One-way ANOVA, $p < 0.9848$, and $p < 0.6151$) by m^{6}A-writers *AeMETTL3* and *AeMETTL14* knockdown when compared to negative control *dsGFP* three days post-transfection (Fig. 3C). However, there was a slight difference (One-way ANOVA, $p < 0.0045$) in *Wolbachia* density between Cellfectin transfection medium-only and *dsGFP* negative control treated cells (Fig. 3C). No reduction (One-way ANOVA, $p < 0.1965$, and $p < 0.7371$) in *Wolbachia* density was also observed following the knockdown of m^{6}A-reader *AeYTHDF3*, and m^{6}A-eraser *AeALKBH8* under the same conditions shown in Fig. 4C.

Despite not observing an effect on *Wolbachia* density following the knockdown of m^{6}A related genes, a study investigating m^{6}A modification on DENV genomic RNA demonstrated that knockdown of m^{6}A-writers and reader *AeYTHDF3* significantly reduced the levels of DENV gRNA and resulted in a decrease of DENV titre [26].

Identification of differential m^{6}A RNA modification

To investigate the m^{6}A methylation status at the single-nucleotide resolution in mRNA, RNA extracted from Aag2.*w*AlbB (average 90 *Wolbachia* per cell) and *Wolbachia*-free Aag2 cells were used for Nanopore direct RNA sequencing (DRS) (Fig. S1). Sequencing runs of 72 h generated between 3.2 and 6.1 and 2.9 to 4.5 million reads for cells persistently infected with the *w*AlbB strain of *Wolbachia* and *Wolbachia*-free Aag2 cells, respectively (Table S2). The average sequence read length, mean quality score, and other DRS metrics are shown in Table S2. To prepare the DRS data, we aligned the basecalled FASTQ reads to the *Ae. aegypti* (AaegL5.3) reference transcriptome achieving between 94 and 96% alignment with minimap2 (Table S2). We applied the nanopolish eventalign function to group the signal-level data from each read into 5-mer events (five nucleotides in length) and mapped them to their corresponding positions in the *Ae. aegypti* transcriptome. For the detection of differential m^{6}A RNA modification, the xPore tool was used [101]. The 3rd position (NNANN) in a 5-mer was chosen

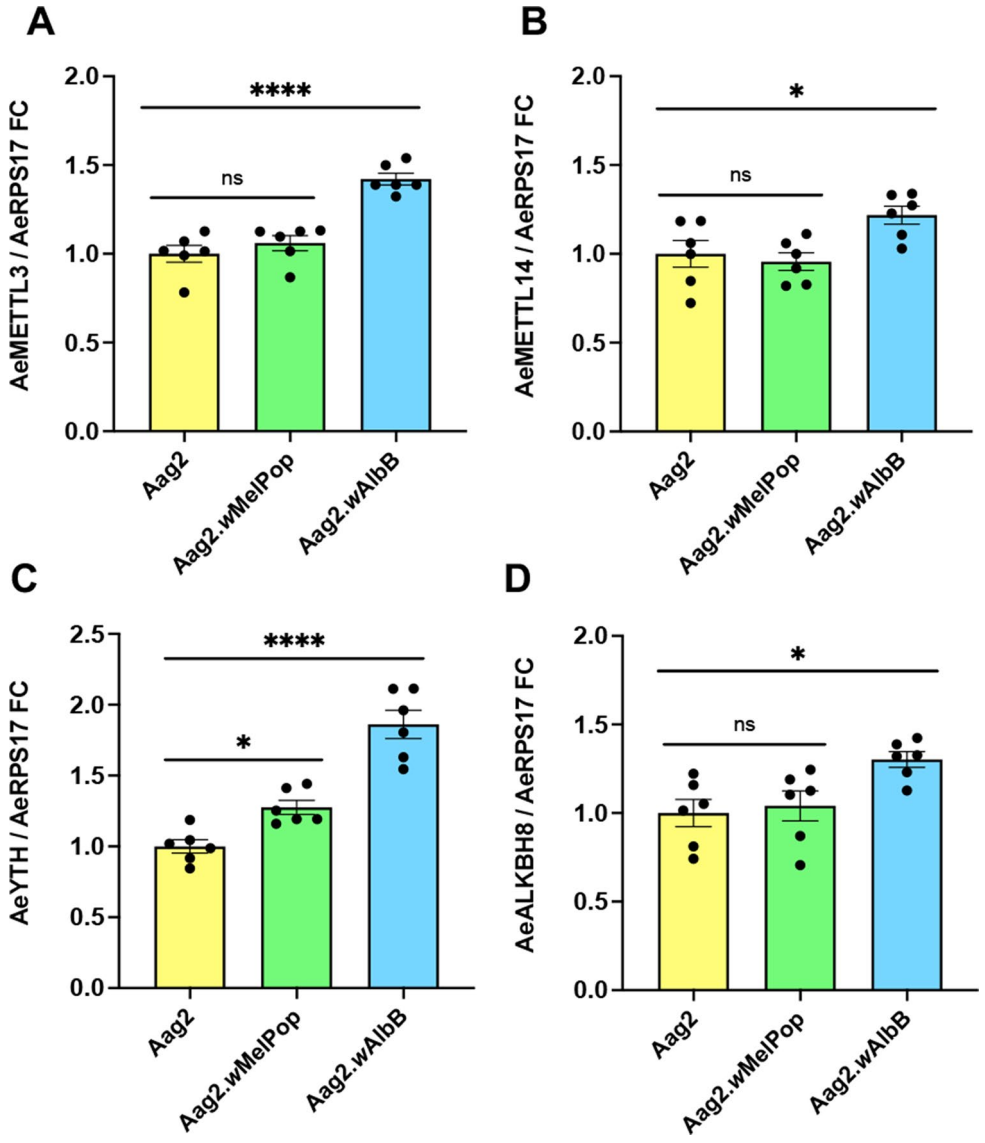

Fig. 2 Differential expression of m^{6}A methylation-related genes in Aag2, Aag2.*w*MelPop, and Aag2.*w*AlbB cells. The relative expression of (**A**) *AeMETTL3*, (**B**) *AeMETTL14*, (**C**) *AeYTHDF3*, and (**D**) *AeALKBH8* in Aag2, Aag2.*w*MelPop, and Aag2.*w*AlbB cells was measured using RT-qPCR, respectively. *Ae. aegypti ribosomal protein S17* (*RPS17*) gene was used as the normalizing gene. One-way ANOVA with Dunnett's *post-hoc* multiple comparison tests was performed to determine statistical significance between groups where each data point represents three biological replicates from two independent experiments and cell line passages. All gene expression levels were adjusted to 1 and expressed as fold changes relative to controls. The error bars represent the standard error of the mean (SEM) of the six biological replicates for each condition. Asterisks denote statistical significance, ns, not significant; *, $p < 0.05$; ****, $p < 0.0001$. FC, fold change

to identify m^{6}A modifications based on studies showing that the signal intensity of the centre nucleotide showed the strongest difference between predicted modified and unmodified sites, and with dwell time showing the smallest difference [m^{6}Anet Fig. 1b [41]], [xPore Fig. 2d and i [101], and EpiNano Fig. 2a [72]]. The detailed steps of Nanopore DRS analysis categorised into pre-process, input/output data files, and post-process are illustrated in Fig. S2. Furthermore, since m^{6}A RNA modification specifically occurs at the DRACH consensus motif (where D = G/A/U, R = G/A and H = U/A/C), we removed any non-DRACH motifs from the dataset.

Transcriptome-wide DRACH motif frequency

Using a differential modification rate (DMR) cut-off of 0.25 and p value < 0.05 resulted in a total of 1,392 differentially modified m^{6}A sites transcriptome-wide. Of these, 776 were associated with increased and 616 with decreased differentially modified m^{6}A DRACH motifs due to *Wolbachia* (Fig. 5A and C, Table S3). Illustrations of the most frequently modified m^{6}A sites for both

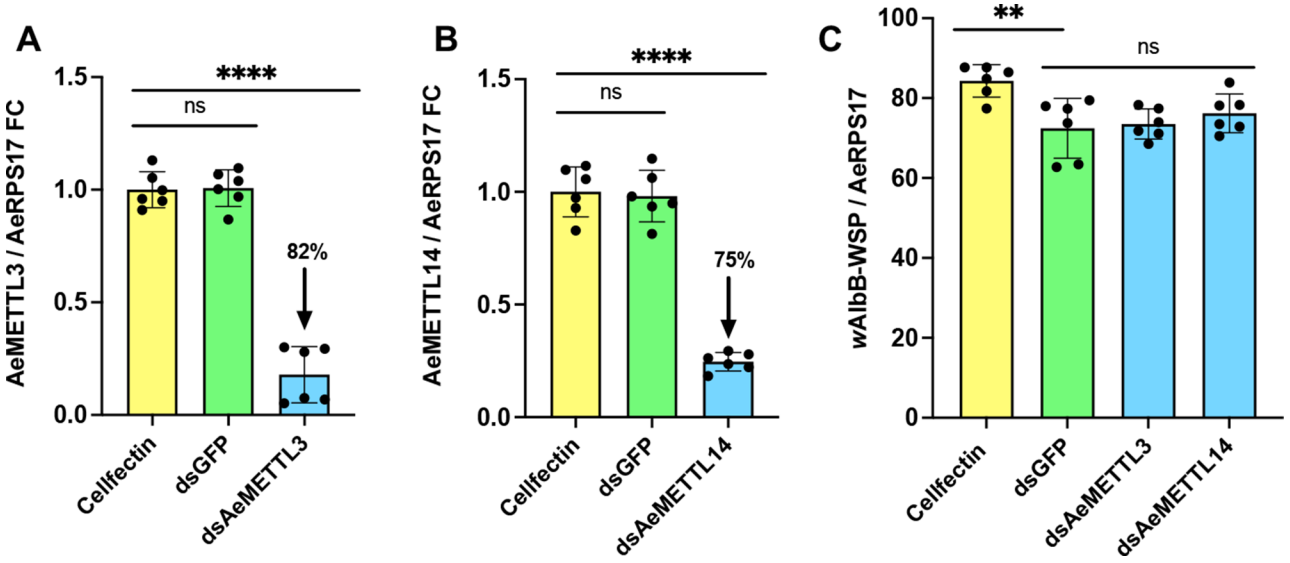

Fig. 3 Double-stranded RNA-mediated knockdown of m^{6}A-writer *AeMETTL3* and *AeMETTL14* does not affect the density of *Wolbachia*. Aag2.*w*AlbB cells were transfected with (**A**) *dsAeMETTL3* or (**B**) *dsAeMETTL14*, and non-targeting *dsGFP*, and Cellfectin transfection reagent only as controls. Three days post double transfection, total RNA was extracted, reverse transcribed, and analysed by RT-qPCR. *Ae. aegypti RPS17* was used as the normalizing gene. (**C**) Relative density of *Wolbachia* following dsRNA knockdown. qPCR analysis of extracted genomic DNA using primers to *Wolbachia*'s *wsp* gene and the host cell *RPS17* gene showed no reduction in *Wolbachia* density following m^{6}A-writer *AeMETTL3*, and *AeMETTL14* dsRNA knockdown when compared to controls 3 days post double transfection. One-way ANOVA with Tukey's *post-hoc* multiple comparison tests was performed to determine the statistical significance between groups. All reported values are relative to non-targeting GFP control. Controls and dsRNA treatments were adjusted to 1. The error bars represent the standard error of the mean (SEM) of six biological replicates for each treatment. Asterisks denote statistical significance, ns, not significant; **, $p < 0.001$, ****, $p < 0.0001$. FC, fold change

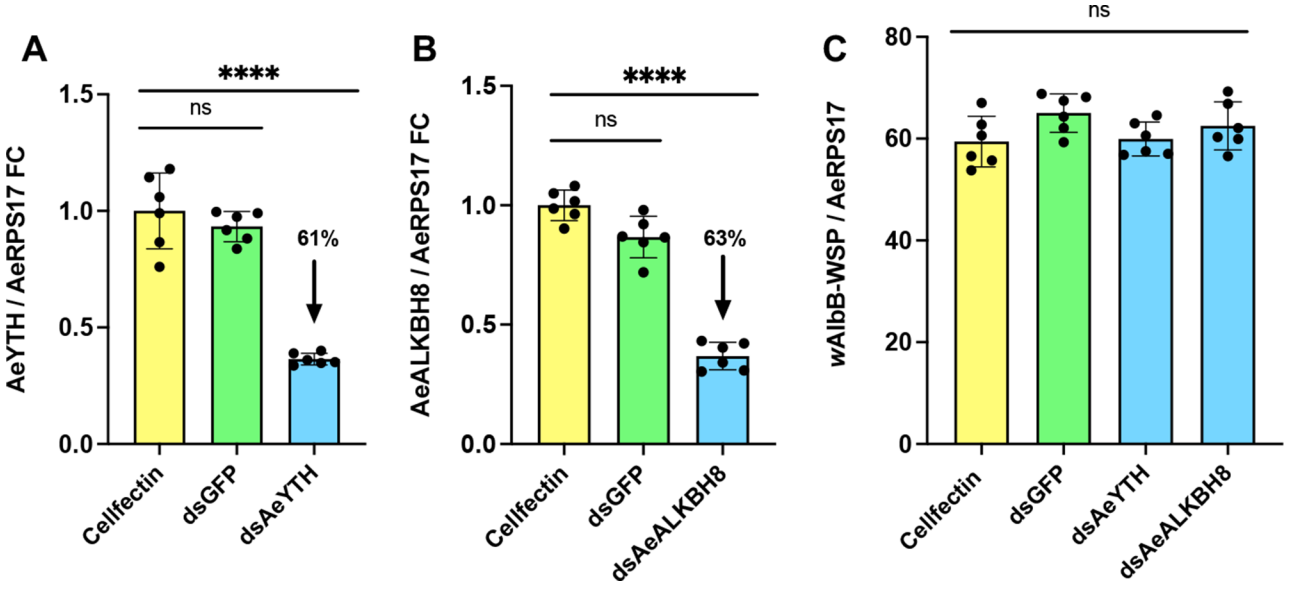

Fig. 4 Double-stranded RNA-mediated knockdown of m^{6}A-reader *AeYTHDF3* and m^{6}A-eraser *AeALKBH8* does not affect the density of *Wolbachia*. Aag2.*w*AlbB cells were transfected with (**A**) *dsAeYTHDF3*, (**B**) AeALKBH8, and non-targeting *dsGFP*, and Cellfectin transfection reagent only as controls. Three days post double transfection, total RNA was extracted, reverse transcribed and analysed by RT-qPCR. *Ae. aegypti RPS17* was used as the normalizing gene. (**C**) Relative density of *Wolbachia* following dsRNA knockdown using *dsAeYTHDF3*, *dsAeALKBH8*, non-targeting dsGFP, and Cellfectin transfection reagent only as controls shown in A and B. qPCR analysis of extracted genomic DNA using primers to *Wolbachia's wsp* gene and the host cell *RPS17* gene showed no reduction in *Wolbachia* density following m^{6}A-reader *AeYTHDF3* and m^{6}A-eraser *AeALKBH8* dsRNA knockdown when compared to controls 3 days post double transfection. One-way ANOVA with Tukey's *post-hoc* multiple comparison tests was performed to determine the statistical significance between groups. The error bars represent the standard error of the mean (SEM) of six biological replicates. Asterisks denote statistical significance, ns, not significant; ****, $p < 0.0001$. FC, fold change

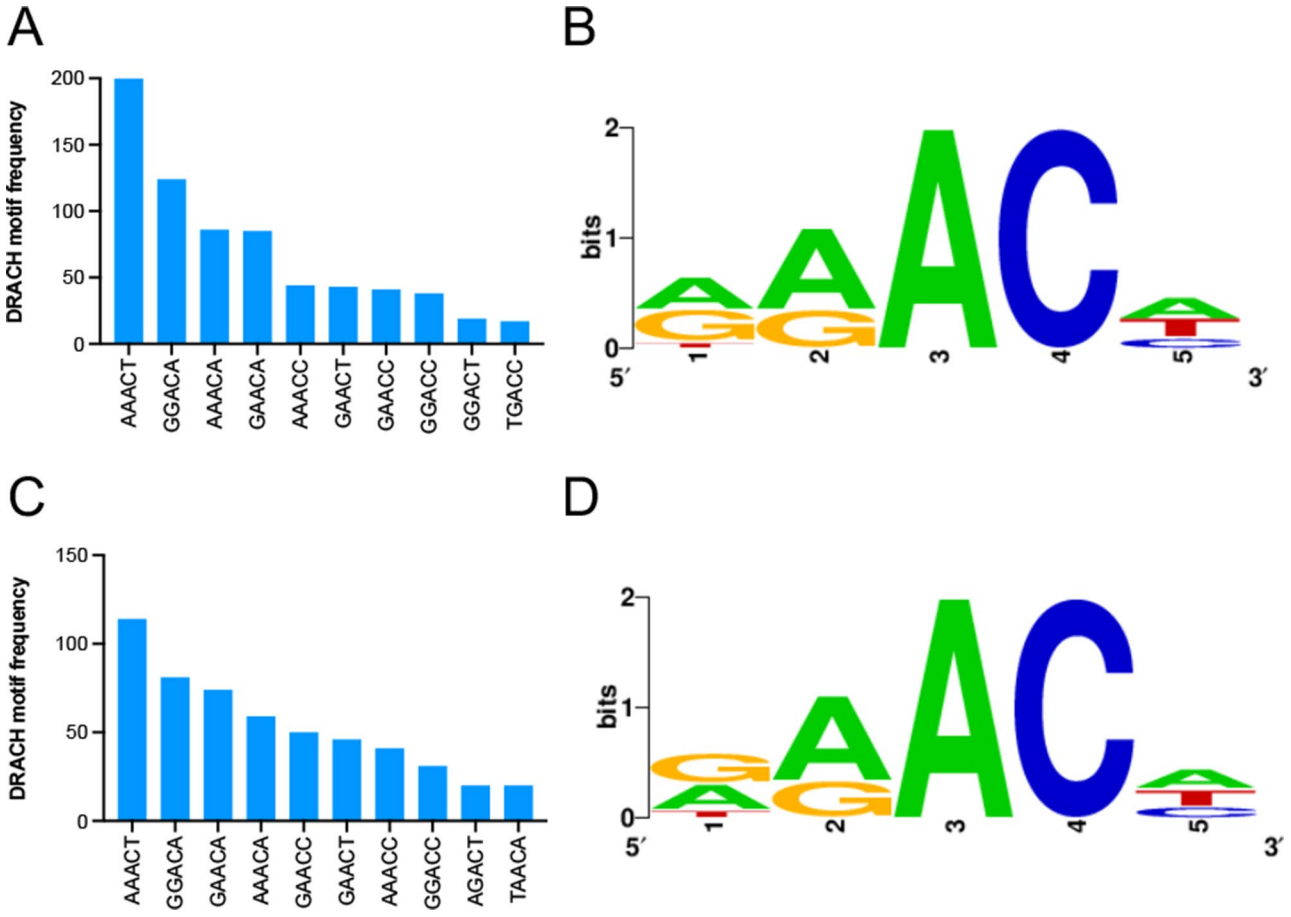

Fig. 5 Transcriptome-wide DRACH motif frequency of increased and decreased m^{6}A levels due to *Wolbachia*. (**A**) The frequency of the top 10 increased DRACH motifs at significantly differentially modified positions based on differential modification rates (DMR) 0.25 from the total number of 776 sites. (**B**) Most frequently modified DRACH motifs of the 776 sites with increased levels of m^{6}A ($p < 0.05$) and DMR 0.25. (**C**) The frequency of the top 10 decreased DRACH motifs at significantly differentially modified positions based on DMR 0.25 from total numbers of 616 sites. (**D**) Most frequently modified DRACH motifs of the 616 sites with decreased levels of m^{6}A ($p < 0.05$) and DMR 0.25. All m^{6}A modified sites were identified by xPore, and *p* values were calculated from a two-tailed, unpooled *z*-test on the modification-rate difference between *Wolbachia*-transinfected vs. *Wolbachia*-free Aag2 cells and adjusted for multiple comparisons using the Benjamini–Hochberg correction

increased and decreased DRACH motif levels are shown in Fig. 5B and D.

Top significant m^{6}A-modified genes ranked by DMR

Applying DMR cut-off of 0.25 and *p* value < 0.05 identified a total of 1,126 genes with significantly differentially modified m^{6}A DRACH motifs (Table S4A and B). We observed a global increase in m^{6}A modifications due to *Wolbachia* with 620, and 506 genes showing an increase and decrease in modified m^{6}A sites, respectively (Table S4A and B).

Of the top 20 genes containing the highest number of increased m^{6}A DRACH motifs, *Toll-like receptor* (*Toll5A*) (AAEL007619) carried the most, with nine m^{6}A sites being modified, followed by *ATP-binding cassette subfamily A member 3* (AAEL012698) with six sites. The remaining genes contained either five, four, or three m^{6}A sites (Fig. 6A, Table S5). As for the top genes with decreased m^{6}A DRACH motifs, the *elongation of very long chain fatty acids protein baldspot* (AAEL013128) contained eight m^{6}A DRACH motifs, while *vanin-like protein 2* (AAEL025718) contained four. The remaining ones carried all three, except for one gene with two m^{6}A sites present (Fig. 6B, Table S5). Essentially, the majority of differentially m^{6}A-modified genes exhibited fewer than five m^{6}A sites per gene (Fig. 6A and B, Table S5).

m^{6}A DRACH motif sites were highly enriched in the coding sequences (CDS; 56%, 57%), and in the 3′-untranslated regions (3′-UTR; 21%, 18%) in differentially modified m^{6}A positions with increased and decreased levels due to *Wolbachia*, respectively (Fig. 7, Table S7A and S7B). 5′-untranslated regions (5′-UTR) represented 6%, and m^{6}A DRACH motif sites between regions (Others), 17% and 19%, respectively.

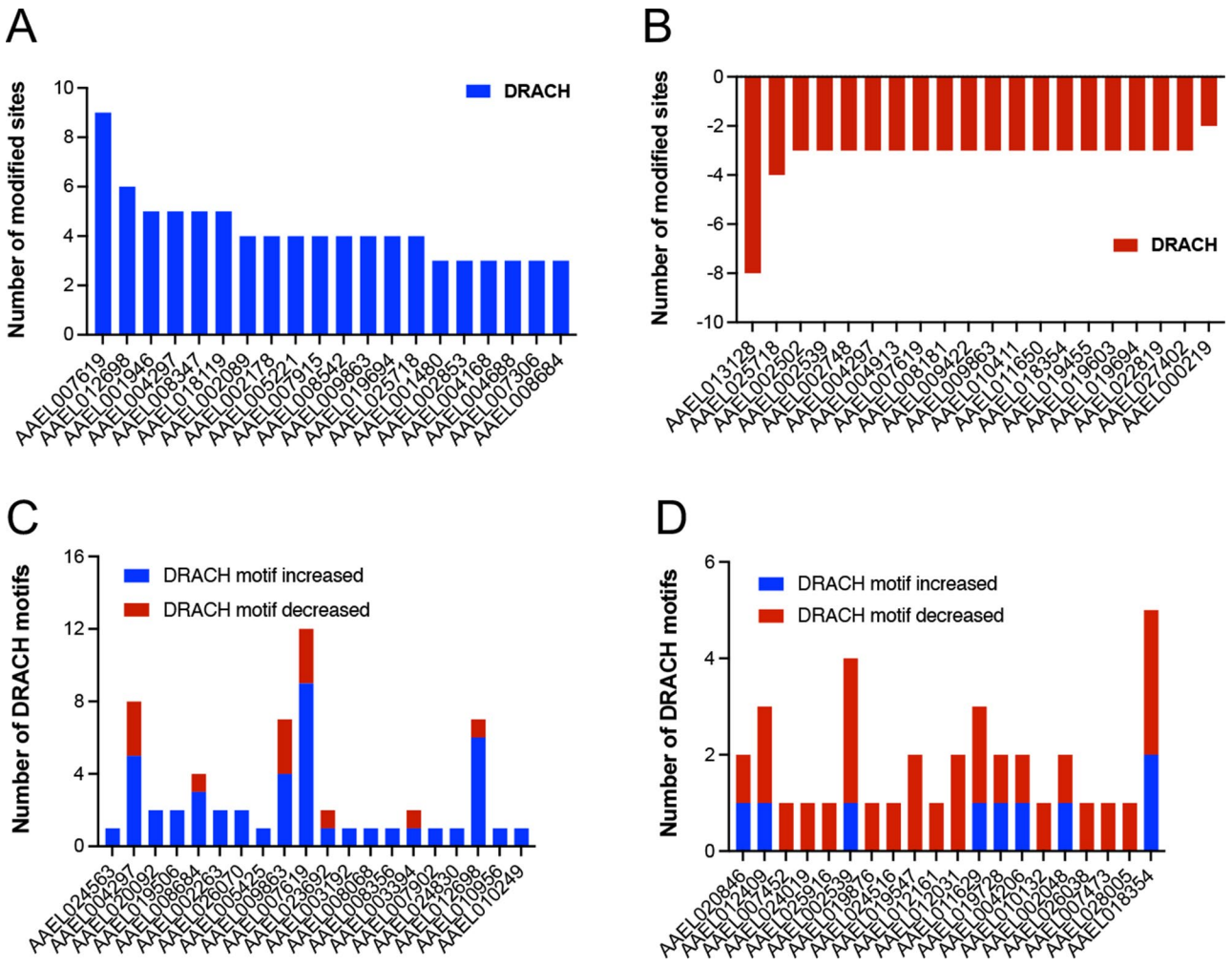

Fig. 6 The number of differentially modified positions in genes ranked by differential modification rate (DMR). (**A**) The top 20 genes were ranked by the total number of increased m^{6}A DRACH motifs, and (**B**) the top 20 genes were ranked by the total number of decreased m^{6}A DRACH motifs due to *Wolbachia*. (**C**) Top 20 genes with positive DMR (increased m^{6}A) ranked by differential modification rate (DMR) including m^{6}A status of increased and decreased DRACH motifs, and (**D**) Top 20 genes with negative DMR (decreased m^{6}A) including m^{6}A status of increased and decreased DRACH motifs due to *Wolbachia*. All significantly differentially modified positions are based on $p < 0.05$ and DMR 0.25 criteria. The m^{6}A DRACH motifs with increased levels are shown in blue, and the m^{6}A DRACH motifs with decreased levels are shown in red

Gene ontology enrichment analysis of the differentially modified m^{6}A genes

The 620 and 506 genes containing differentially modified m^{6}A DRACH motifs were submitted for Gene Ontology enrichment analysis in Blast2GO. A total of 35 and 36 GO terms amongst the combined categories of molecular function, biological process, and cellular component for increased and decreased differentially modified m^{6}A genes were returned, respectively (Table S8A and S8B). The top 30 over-represented GO terms of increased modified m^{6}A sites revealed 17 unique GO terms: binding, metabolic process, primary metabolic process, cellular metabolic process, nucleus, localisation, establishment of localisation, transport, endomembrane system, catabolic process, intracellular transport, catalytic activity-acting on a nucleic acid, cytoplasmic vesicle, intracellular vesicle, vesicle, nucleoside-triphosphatase regulator activity, GTPase regulator activity (Fig. 8A). Similarly, 17 uniquely enriched GO terms were discovered for decreased modified m^{6}A sites carrying genes that are related to cellular component organisation, anion binding, purine nucleotide binding, purine ribonucleoside triphosphate binding, ribonucleotide binding, purine ribonucleotide binding, phosphorus metabolic process, phosphate-containing compound metabolic process, adenyl nucleotide binding, ATP binding, adenyl ribonucleotide binding, cell cycle, cytoskeletal protein binding, protein transport, cell cycle process, intracellular protein transport, supramolecular fibre (Fig. 8B).

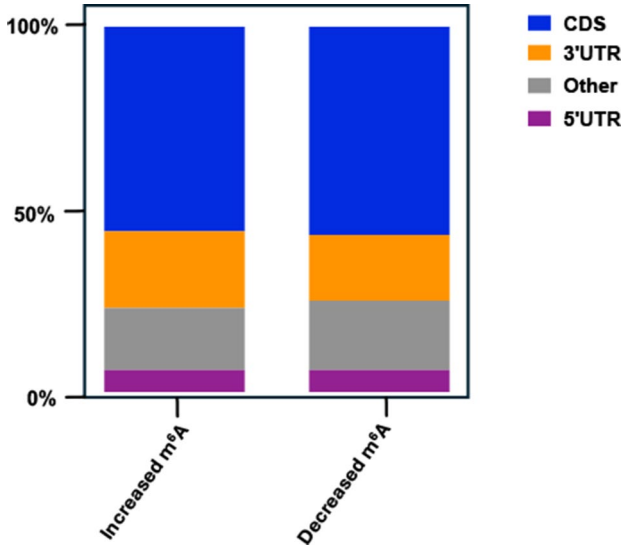

Fig. 7 Genomic locations of m^{6}A DRACH motif sites. Differentially modified m^{6}A motifs were identified at the transcriptome level and mapped to genomic coordinates of the *Ae. aegypti* genome. m^{6}A sites of increased and decreased DRACH motifs due to *Wolbachia* at significantly differentially modified positions based on differential modification rate (DMR) 0.25 and $p < 0.05$. Genomic location names and percentages are depicted within the graph and legend. Coding sequence (CDS), untranslated region (UTR), and m^{6}A DRACH motif sites between regions (Others)

Differential expression of mosquito genes in *Wolbachia*-infected and uninfected cells

A total of 810 protein-coding genes were significantly differentially expressed when comparing Aag2.*w*AlbB to Aag2 cells and considering $\log_2$ fold change ≥ 2 and FDR p value ≤ 0.05 using DESeq2. Of these, 500 (61.7%) were downregulated, and 310 (38.3%) were upregulated (Fig. 9A and C, Table S9A). Furthermore, a total of 174 long non-coding RNA (IncRNA) with 151 (86.8%) down- and 23 (13.2%) upregulated were also identified (Fig. 9B, Table S9B). DEG analysis with CLC-GWB identified roughly similar numbers with a total of 802 differentially expressed protein-coding genes, of which 527 (65.7%) and 275 (34.3%) were down- and upregulated, respely (Fig. 9A and C, Table S9C). In addition, a total of 182 IncRNAs, with 162 (89.0%) down- and 20 (11.0%) upregulated, were also identified (Fig. 9B, Table S9D). Venn diagram of differentially expressed genes identified by DESeq2 and CLC-GWB showed an overlap of 643 (66.4%) genes (Fig. 9C, Table S9E). Of these overlapping DEGs, 427 (66.4%) were downregulated, and 216 (33.6%) were upregulated (Table S9E).

A representative selection of nine differentially expressed *Ae. aegypti* genes identified by differential gene analysis using DESeq2 and CLC were validated by RT-qPCR. The results showed an overall consistency between Nanopore DRS read counts and RT-qPCR, when DEGs in Aag2 and Aag2.*w*AlbB cells were considered (Fig. 10).

Principal-component analysis (PCA) showed a significant difference in variance between *Wolbachia*-transinfected Aag2.*w*AlbB and *Wolbachia*-free Aag2 samples, demonstrating a high level of similarity among

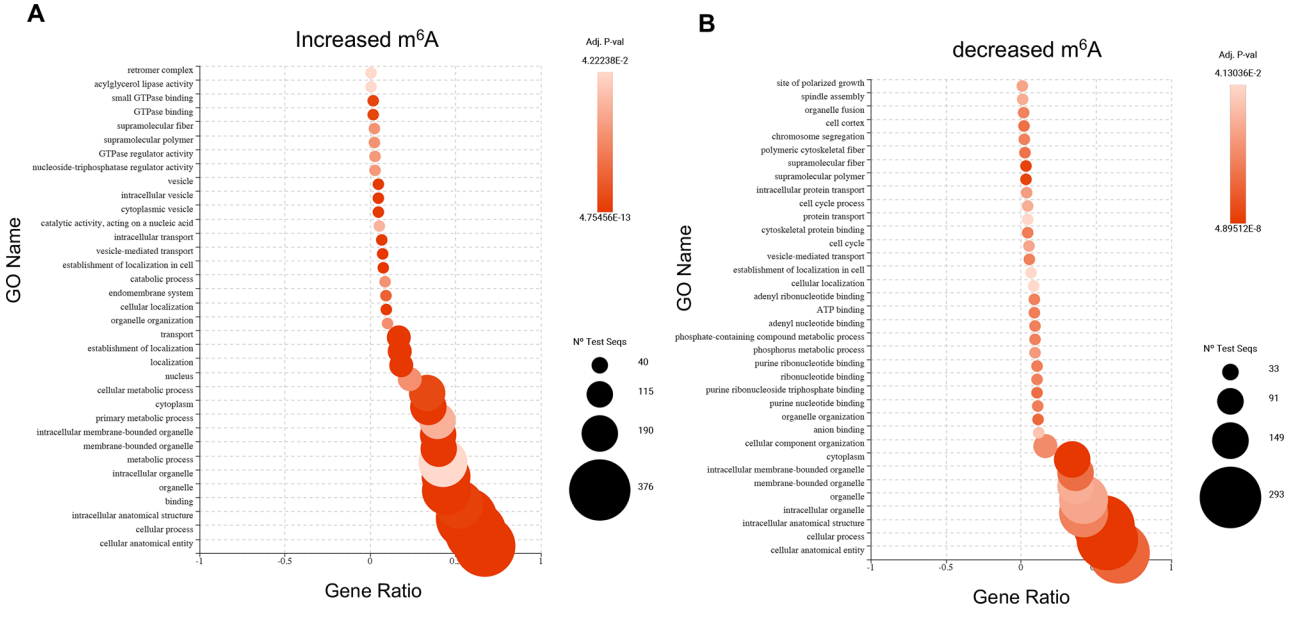

Fig. 8 Gene Ontology (GO) enrichment analysis of m^{6}A DRACH motif enriched genes. The data represents the combined Gene Ontology term categories of biological process, molecular function, and cellular component for over-represented terms of (**A**) 620 genes containing differentially modified m^{6}A DRACH sites increased and (**B**) 506 genes containing differentially modified m^{6}A DRACH sites decreased due to *Wolbachia* at significantly differentially modified positions based on differential modification rate (DMR) 0.25 and $p < 0.05$. Point size represents the number of enriched genes in each term, and the red-coloured scale indicates the significance by p value

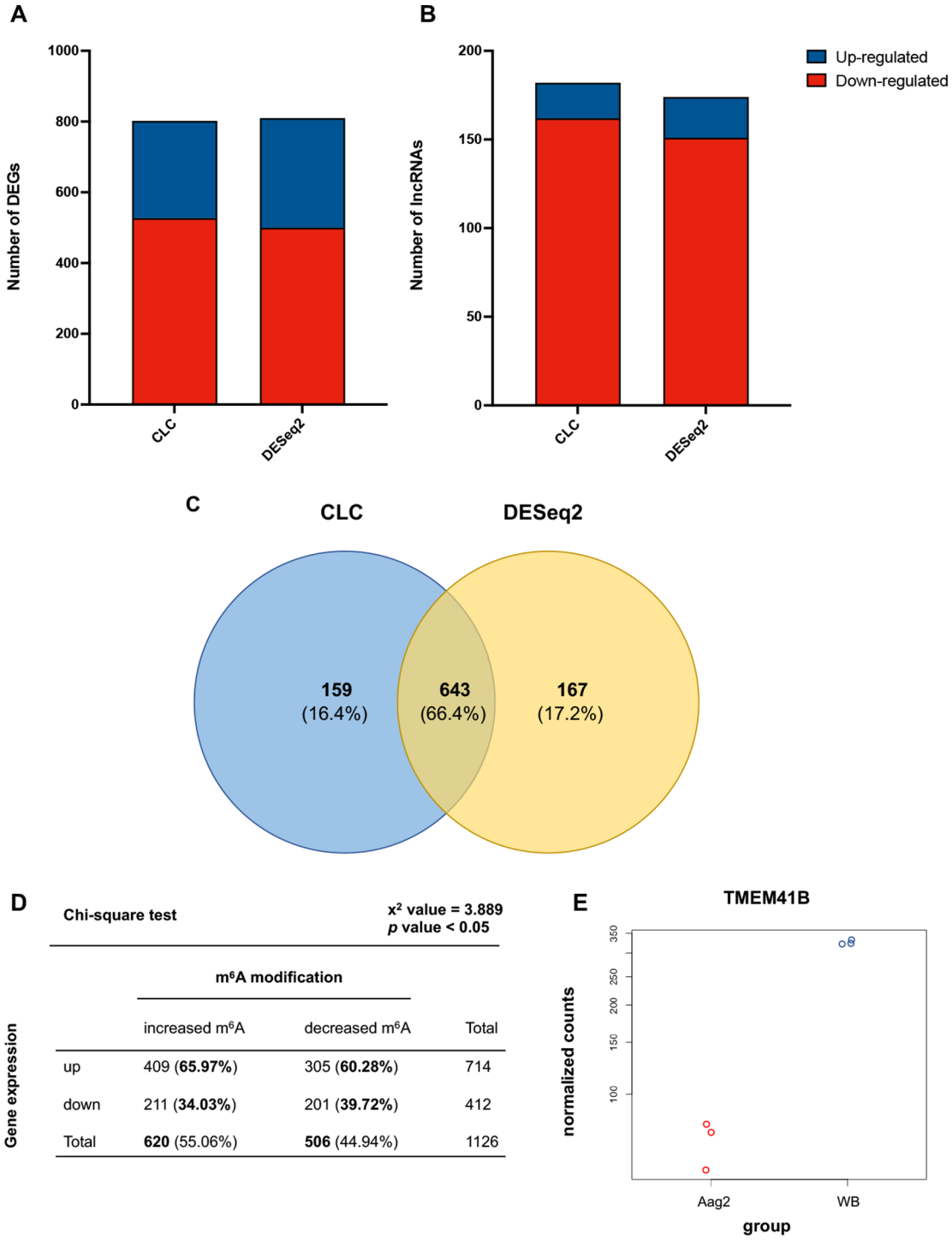

Fig. 9 Differentially expressed protein-coding genes (DEGs) and long non-coding RNAs (lncRNAs) between Aag2 and Aag2.*w*AlbB cells. The bar graphs show the number of (**A**) DEGs and (**B**) lncRNAs identified using CLC-GWB and DESeq2. Parameters of $\log_2$ fold-change of ≥ 2.0 and an adjusted *p* value of < 0.05 were applied. (**C**) Venn diagram showing DEGs identified with CLC-GWB versus DESeq2. (**D**) Chi-Square test of differentially modified m^{6}A genes and their respective gene expression levels. (**E**) TMEM41B normalized counts

the biological replicates (Fig. S3A, B). The first and second principal components described 93% and 64% of the variance for mapped reads analysed with DESeq2 and CLC-GWB, respectively.

We also performed a conjoint analysis of the differentially modified m^{6}A genes and their respective gene expression levels to see whether the m^{6}A modifications' status affects gene expression. The chi-square test

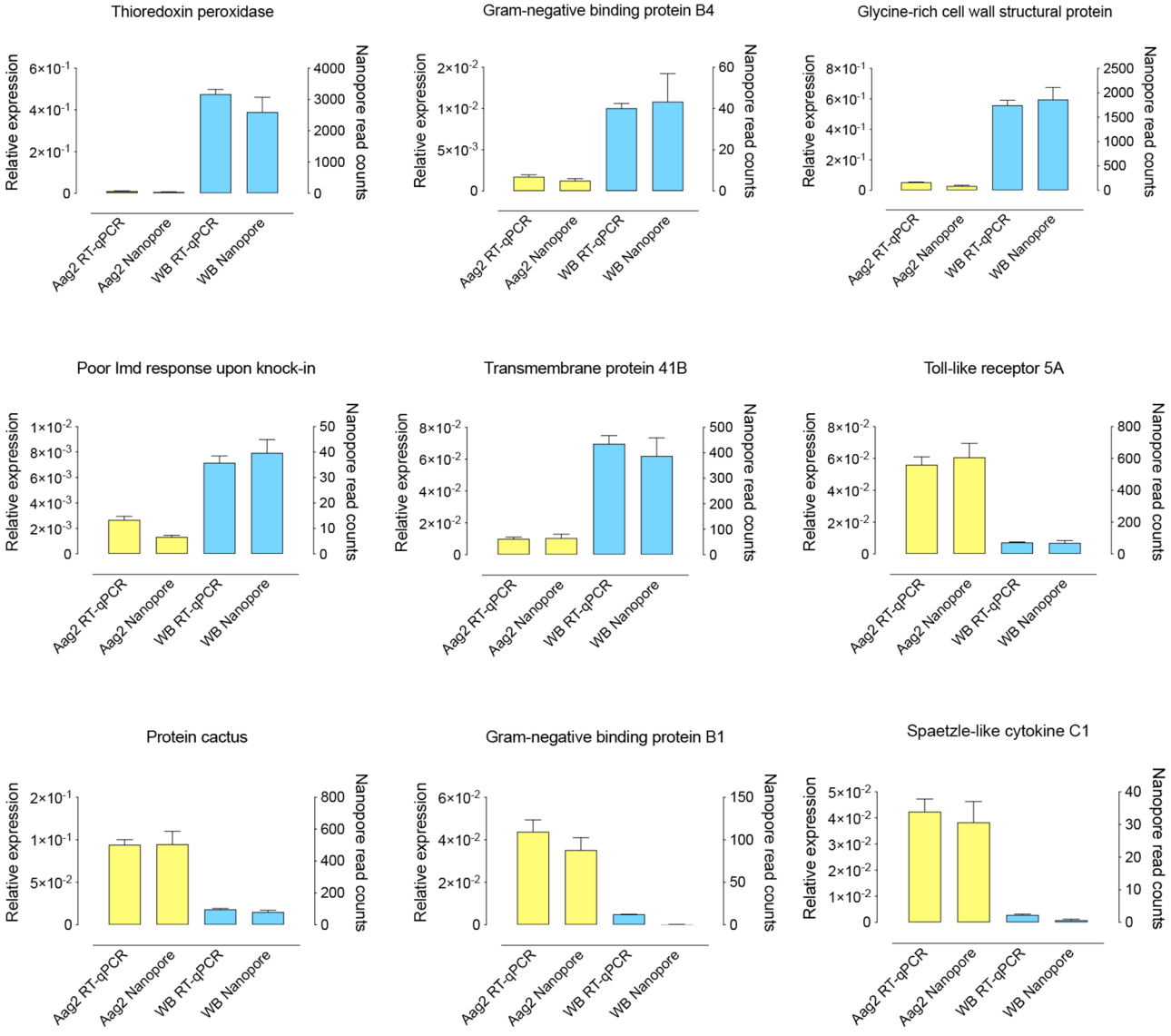

Fig. 10 Validation of differentially expressed mosquito genes. The bar graphs represent the Nanopore direct RNA sequencing read counts and RT-qPCR relative expression results of the differentially expressed genes in Aag2 and Aag2.*w*AlbB cells. The error bars represent the standard error of the mean (SEM) of three biological replicates

showed an overall upregulation of gene expression in genes with increased and decreased levels of m^{6}A modification (Fig. 9D, Table S10A-C). *TOLL5A*, the gene with the largest increase of nine m^{6}A modifications due to *Wolbachia*, was downregulated by several magnitudes ($\log_2$FC = -3.49) as shown in Fig. 6A. Whereas *baldspot*, the gene with the largest decrease of eight m^{6}A modifications due to *Wolbachia*, was upregulated ($\log_2$FC = + 1.08) as shown in Fig. 6B. Additionally, a gene encoding a *transmembrane protein 41B* (*TMEM41B*), which is a critical host factor required for flavivirus infection, was also present among the upregulated ($\log_2$FC = + 2.22) differentially expressed genes (Fig. 9E, Table S9E). Interestingly, *TMEM41B* contained an increase of three m^{6}A modifications due to *Wolbachia* (Table S9A).

Wolbachia infection increased the expression of *TMEM41B* in Aag2.*w*MelPop (One-way ANOVA, $p < 0.0049$), and Aag2.*w*AlbB (One-way ANOVA, $p < 0.0001$) cells when compared to Aag2 cells (Fig. 11A). To further determine whether *TMEM41B* affects DENV replication, we knocked down *TMEM41B* in Aag2 cells using dsRNAs and infected the cells with DENV. RT-qPCR was performed on RNA extracted from cells collected at 2 days post-infection (dpi), confirming the effective knockdown of *TMEM41B* (83%) (Fig. 11B). *TMEM41B* depletion significantly decreased (~ 2-3-fold; $p < 0.0019$) the levels of DENV genomic RNA (Fig. 11B and C). Our results of reduced DENV gRNA following the knockdown of *TMEM41B* are consistent with research conducted with knocked out and reconstituted

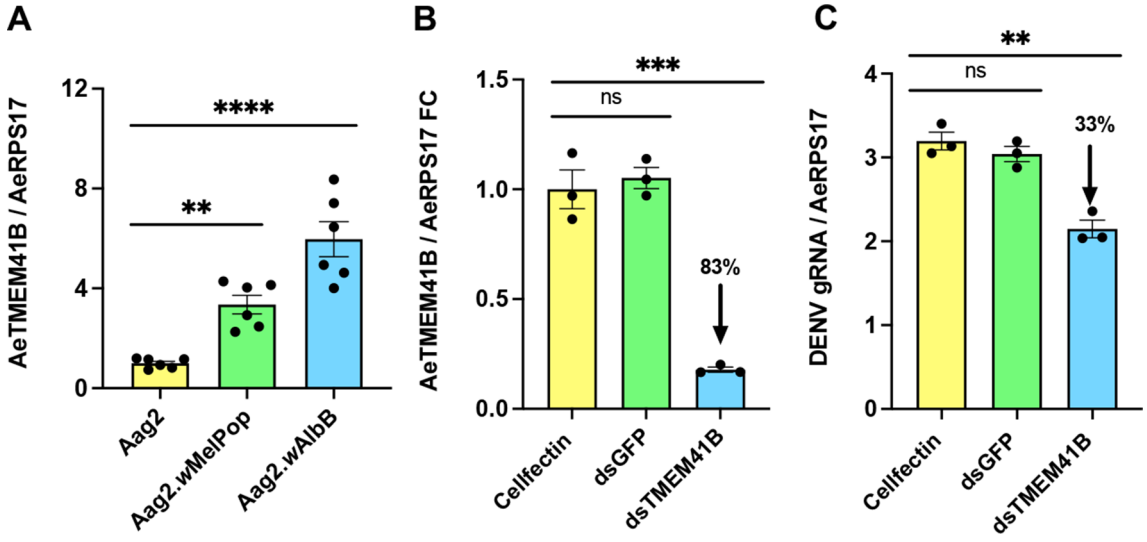

Fig. 11 *Wolbachia* infection increased gene expression of *TMEM41B* and double-stranded RNA-mediated knockdown of *TMEM41B* decreased the levels of DENV genomic RNA. (**A**) Relative expression of *TMEM41B* in Aag2, Aag2.*w*MelPop, and Aag2.*w*AlbB cells was measured using RT-qPCR. (**B**) and **(C)** Reduction in DENV genomic RNA in Aag2 cells following dsRNA knockdown. Aag2 cells were double transfected with *dsTMEM41B*, non-targeting *dsGFP*, and Cellfectin transfection reagent only as controls. Cells were collected at 2 dpi, for RNA extraction and quantification of *TMEM41B* expression (**B**), and for DENV genomic RNA by RT-qPCR (**C**). *Ae. aegypti RPS17* was used as the normalizing gene. One-way ANOVA with Tukey's *post-hoc* multiple comparison tests was performed to determine the statistical significance between groups. The error bars represent the standard error of the mean (SEM) of the biological replicates. Asterisks denote statistical significance, ns, not significant; $^{**}p < 0.01$; $^{***}p < 0.001$; $^{****}p < 0.0001$. FC, fold change

mosquito *TMEM41B* ortholog in Aag2 (*Ae. aegypti*) and C6/36 (*Ae. albopictus*) mosquito cells [43]. They found that infection rates of DENV and other flaviviruses were decreased by 41–67% following the knockout of *TMEM41B*, and found that *TMEM41B* was required as a host factor in various virus-cell combinations such as CHIKV, DENV, WNV, YFV, and ZIKV [43].

Gene ontology for DEGs

Gene Ontology (GO) enrichment analysis of down- and upregulated DEGs was performed using Blast2GO (Fig. 12A and B, Table S11A and B). This analysis identified 191 combined GO terms amongst the categories of biological process, molecular function, and cellular component. The top 30 over-represented GO terms of down-regulated DEG's include catalytic activity, serine-type endopeptidase activity, defense, defense response to bacterium and other organisms, innate immune response, regulation of immune response, and cellular process, and cellular biosynthetic processes. For the upregulated group, a total of 6 GO terms were over-represented, which included glutathione catabolic process, glutathione hydrolase activity, threonine-type peptidase activity, omega peptidase activity, heat shock-mediated polytene chromosome puffing, polytene chromosome puffing.

Discussion

Previous studies reported *Wolbachia*'s ability to alter the expression of *Ae. aegypti*'s arginine methyltransferase [138], and cytosine methyltransferase in *Drosophila* and mosquito cells [12–14, 139]. In our previous investigation, we found genes encoding adenosine (m^6A) and cytosine (m^5C) methyltransferases involved in post-transcriptional modifications were elevated at the early hours of dengue virus (DENV) infection in *w*AlbB strain of *Wolbachia*-transinfected *Ae. aegypti* mosquito cells [65]. However, the expression of adenosine methyltransferase and its role in the post-transcriptional landscape in the presence of *Wolbachia* has not been explored. This present study identified m^6A methyltransferase machinery-associated genes to be elevated in *Wolbachia w*AlbB strain-transinfected cells. However, Aag2.*w*MelPop-transinfected cells showed no change in gene expression for m^6A-writers *AeMETTL3*, *AeMETTL14*, and m^6A-eraser *AeALKBH8*. The m^6A-reader *AeYTHDF3* was the only m^6A machinery component with a significant increase in expression in Aag2.*w*MelPop cells. Given the dynamic nature of m^6A methylation, YTH domain-containing family protein 3 (YTHDF3) m^6A-readers located within the cytoplasm have been shown to bind to m^6A-modified mRNAs selectively and to facilitate translation and decay of modified target transcripts in HeLa cells [110, 111]. In fact, *YTHDF3* is the first reader to interact with m^6A modified mRNAs and its binding facilitates the access to *YTHDF1* and *YTHDF2* that promote translation and degradation, respectively [110]. In addition, cytoplasmic YTHDF1-3 proteins can be relocated to the nuclei of cells by stimuli such as heat shock stress and viral infection [39, 111, 143].

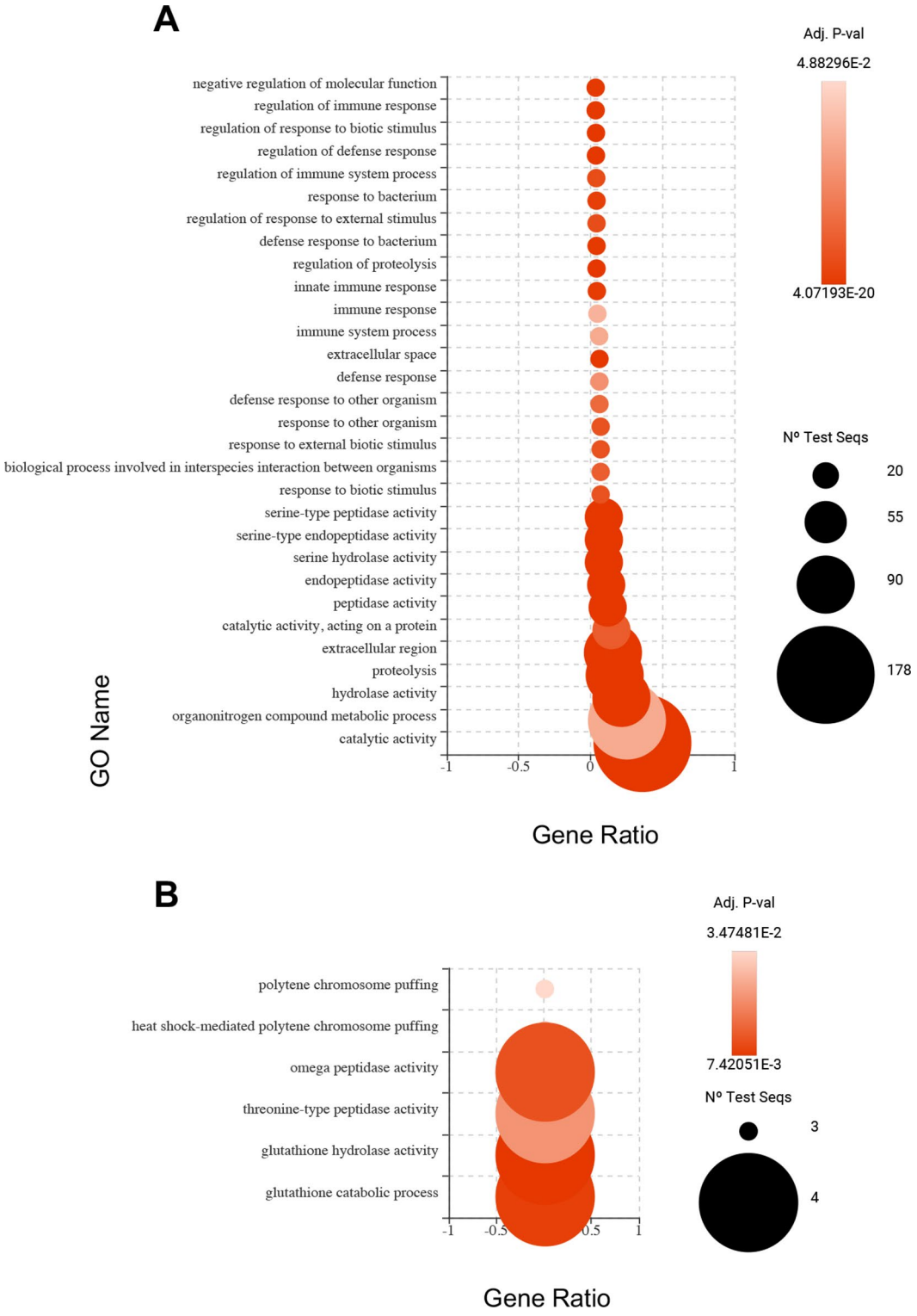

Fig. 12 Gene Ontology (GO) enrichment analysis of down- and upregulated DEGs in *Wolbachia*-transinfected cells. The data represents the combined Gene Ontology term categories of biological process, molecular function, and cellular component for over-represented terms of (**A**) down and (**B**) up-regulated DEGs due to *Wolbachia*. (**A**) In total, 179 GO terms were identified for downregulated, with 104 being over- and 75 terms under-represented. (**B**) A total of 12 GO terms were identified for upregulated DEGs with six being over- and six terms under-represented. Point size represents the number of enriched genes in each term, and the red-coloured scale indicates the significance by *p* value

Other studies have also shown contrasting gene expression levels. For example, arginine methyltransferase was upregulated in Aag2.*w*MelPop-transinfected Aag2 *Ae. aegypti* cells [138]. However, the same strain of *Wolbachia* significantly suppressed the expression of *AaDnmt2*, the gene encoding cytosine methyltransferase in Aag2.*w*MelPop mosquito cells [139]. The same pattern of reduced AeDnmt2 expression was observed in *Aedes albopictus* mosquito cells colonized with either *w*AlbB or *w*Mel strain of *Wolbachia* [14]. This was the opposite and resulted in increased *Dm* DNMT2 expression in a *Drosophila melanogaster* cell line transinfected with *Wolbachia* strain *w*Mel [12]. Evidently, different strains of *Wolbachia* and host combinations confer certain characteristics. Our results showed that knocking down the individual host m^{6}A-writers, -reader, and -eraser genes using dsRNA did not affect *Wolbachia* density three days post-transfection. Conversely, knockdown of m^{6}A-writers and reader *AeYTHDF3* in virus-infected Aag2 cells significantly reduced the levels of DENV gRNA and resulted in a decrease of DENV titre [26].

Nanopore direct RNA sequencing (DRS) identified a total of 1,392 high-confidence differentially modified m^{6}A sites in 1,126 genes. Of these DRACH motif methylated sites, 776 and 616 showed increased and decreased m^{6}A level abundance within 620 and 506 genes due to *Wolbachia*, respectively. Our total number of detected differentially methylated m^{6}A sites and genes is lower than other studies using Nanopore sequencing and xPore in human cell lines, cancer tissues, and *Arabidopsis* [101, 134]. The study in human HEK293T and clinical myeloma cells identified a total of 4,447 differentially modified positions [101]. Researchers conducting work in *Arabidopsis thaliana* found a total of 3,459 differentially methylated m^{6}A sites in 2,068 protein-coding genes [134]. What both studies have in common is that their detection focused on the A-centred k-mers (NNANN) reporting modification results for non-DRACH and DRACH motifs, using a $p < 0.05$ but no differential modification rate cut-off. However, we also adopted the A-centred k-mer (NNANN) approach in our initial detection step followed by selectively filtering our data for m^{6}A DRACH consensus motifs, therefore removing all non-DRACH modifications from the dataset, used $p < 0.05$, and applied a DMR cut-off of 0.25. Exclusively selecting for m^{6}A DRACH motifs and applying a more stringent DMR cut-off criteria provides a reasonable explanation for the difference in total numbers of m^{6}A modified sites being reported.

Most of the differentially m^{6}A-modified genes contained fewer than five m^{6}A sites per gene. The gene with the largest increase of nine m^{6}A modifications due to *Wolbachia* was a Toll-like receptor (*Toll5A*) (AAEL007619). In contrast, the gene with the largest decrease of eight m^{6}A modifications due to *Wolbachia* was an *elongation of very long chain fatty acids protein baldspot* (AAEL013128). Toll-like receptors such as Toll5A are part of and link extracellular immune signals to the Toll intracellular transduction pathway [63, 112]. Toll5A is known for its immune sensory function and as a receptor that recognises bacterial flagellin [5, 107]. The ATP-citrate synthase gene encodes an enzyme involved in the biosynthesis of the essential metabolite acetyl-coenzyme A (CoA), which is a critical building block for fatty acids, cholesterol, and protein acetylation [120]. Acetylation is the major process of post-translational protein modifications within eukaryotic cells [28, 132]. *Indy* encodes a citrate transporter located within the cell plasma membrane. Its function as a longevity gene with the ability to regulate metabolic processes was originally discovered in *D. melanogaster* [96, 130]. Ced-6 was identified as an adaptor protein that mediates intracellular signals during phagocytosis, leading to the engulfment of apoptotic cells [114]. *Vnn2*, the gene with the same number of differentially modified m^{6}A DRACH sites, is known to encode a membrane-associated enzyme active in coenzyme A synthesis [50].

The top 20 genes ranked by the greatest differential modification rate difference showed that genes with positive DMR contained more increased m^{6}A DRACH motifs, whereas the genes with negative DMR had more decreased m^{6}A DRACH motifs present. We also looked at the expression levels of these genes to see if there is a clear correlation between a gene's expression and m^{6}A modification status. Of the genes with increased m^{6}A DRACH motifs levels, 12 (60%), and eight (40%) were up- and downregulated, respectively. For the genes with decreased levels of m^{6}A DRACH motifs, an identical number of genes showed up- and downregulation, 10 (50%), and 10 (50%), respectively. Additionally, we performed a conjoint analysis on the global differentially modified m^{6}A genes and their respective gene expression dataset to see whether there is a clear trend between the m^{6}A modification status and gene expression. Indeed, there is a strong correlation between gene expression being upregulated by 65.97% and 60.28% in genes with both increased and decreased levels of m^{6}A modification, respectively. The percentages from the conjoint analysis of differentially modified m^{6}A genes and their gene expression levels are comparable to values observed by a study in human renal carcinoma cells [70]. The authors performed a Chi-squared test on 5,224 genes to investigate the association between aberrant m^{6}A modification and differential gene expression. They reported that genes with increased m^{6}A levels showed 59.5% unregulated and 40.5% downregulated gene expression [70]. For genes with decreased m^{6}A levels, 56.8% exhibited

unregulated and 43.2% for downregulated gene expression, respectively [70].

To further investigate the functionality of the m^{6}A modifications on genes, we performed Gene Ontology enrichment analysis on the 620 genes with increased and the 506 genes with decreased m^{6}A DRACH motifs levels. Interestingly, genes with reduced differentially modified m^{6}A DRACH motifs due to *Wolbachia* revealed several GO terms associated with purine (adenine and guanine) nucleotide binding, purine ribonucleoside, triphosphate binding, purine ribonucleotide binding, ribonucleotide binding, adenyl nucleotide binding, adenyl ribonucleotide binding, anion and ATP binding being over-represented.

Taken together, the results indicate that lower levels of m^{6}A DRACH motifs favour gene stability and increase functions critical in the post-transcriptional modification process of m^{6}A. This and the fact that m^{6}A modifications can regulate gene expression is backed by research suggesting that the addition or removal of m^{6}A methylations on mRNA can enhance or destabilise transcript stability, consequently altering gene expression levels and promoting or impeding translation efficiency [44, 110, 111, 124, 140]. In terms of genomic coordinates context, m^{6}A DRACH sites were highly enriched in coding sequences (CDS) and 3′-UTR regions and, to a lesser extent, in the 5′-UTR regions in *Wolbachia*-transinfected Aag2.*w*AlbB cells. A recent study discovered a previously unknown pathway and revealed that the location of the m^{6}A modification in the coding sequence triggers mRNA degradation via CDS-m^{6}A decay (CMD) [144]. This supports our findings of m^{6}A DRACH sites being highly enriched in coding sequences and highlights the importance of the m^{6}A location and influence on transcript stability. The abundance of m^{6}A sites predominately within the CDS and 3'UTR is a scenario commonly observed in human and mouse cells [45, 73, 89, 111]. Meyer et al. [89] found that the majority of m^{6}A peaks were present in CDS (50.9%), 3'UTR (37.7%), and 5'UTR (4.2%). In addition, they reported that two-thirds of 3′ UTRs with m^{6}A peaks also contained at least one predicted microRNA-binding site [89]. The 3′ UTR of mRNAs is a crucial region that contains regulatory elements involved in mRNA processing, mRNA stability, subcellular localization, translation regulation/initiation, and microRNA-binding sites [58, 89, 108, 119, 124]. However, most of these studies used antibody-based methods such as methylated RNA immunoprecipitation sequencing (MeRIP-Seq) to detect modified sites. We used Nanopore direct RNA sequencing that reads continuous native mRNA and a computational method called xPore, which removes the requirement of an experimentally generated unmodified control sample (knockout control) to identify differentially modified positions. xPore models a mixture of two Gaussian distributions corresponding to unmodified and modified RNA [101]. In addition, it uses prior information relating to the theoretical signal distribution to guide the Gaussian parameters with means and variances of these two distributions to be shared across samples [101]. Furthermore, the authors evaluated their algorithm against six cell lines and multiple patient samples, reporting high accuracy of predicted modified sites. A recent and comprehensive study evaluated 10 computational tools, including xPore, for the identification of RNA modifications from Nanopore direct RNA-Seq data [115]. Sindbis virus (SINV) RNA isolated from mammalian or mosquito cells with in vitro-transcribed RNAs serving as modification-free control was used to test these tools. xPore was one of the two current signal-based methods to detect most m^{6}A-modified sites accurately.

We also performed DEG analysis utilising the existing Nanopore DRS data to uncover the effect of *Wolbachia* on the mosquito host at the transcriptome level as it has not previously been done with long-read Nanopore sequencing data. We used DESeq2, an R package-based method, and the recently released CLC RNA-Seq analysis package with a long-read support beta tool. Amongst the commonly downregulated DEGs were cellular, catalytic activity, and predominately classical and non-classical immune-related genes. Notably, genes coding for cactus (AAEL000709), Toll-like receptor Toll5A (AAEL007619), spaetzle-like cytokine 1 A (AAEL013433), spaetzle-like cytokine 1 C (AAEL013434), Gram-negative Binding Protein (GNBPB1) (AAEL003889), clip-domain serine proteases (CLIP-SPs), serine protease inhibitor (serpins), antimicrobial peptides (AMPs) such as cecropin (AAEL029047), defensin A (AAEL003841), defensin C (AAEL003832), and cytochrome P450 (CYP450), and leucine-rich proteins.

Cactus, spaetzle-like cytokines, GNBPB1, and Toll-like receptor are core components of the Toll signalling pathway [63]. Cactus is a negative regulator of the Toll pathway, whereas spaetzle-like cytokine molecules activate Toll-like receptors [99]. A recent study in *Ae. aegypti* mosquito showed that spaetzle1C and Toll5A intercalate, and their binding promotes immune signalling [107]. Our data revealed in the presence of *Wolbachia cactus*, *spaetzle1A*,*1 C*, *Toll5A*, sixteen *CLIP-SPs*, and six *serpins* were all downregulated. Given that the critical negative regulator *cactus* is downregulated, this could suggest that the Toll pathway is, in turn, induced. A study conducted in *w*AlbB-transinfected Aag2 cells supports this as it showed when both *cactus* and *caspar*, the respective negative regulators of the Toll and immune deficiency (IMD) pathways, were induced by dsRNA silencing, *Wolbachia* density increased significantly [97]. Likewise, *cecropin* and *defensin*, as known AMPs and part of the mosquito innate immune response, were also downregulated [121,

127]. AMPs can directly target and lyse bacterial membranes, defending against a broad spectrum of invading microorganisms [93, 121, 127]. Overexpression of cecropin and defensin in *Ae. aegypti* mosquitoes strongly inhibited the parasite *Plasmodium* and pathogenic bacteria [61].

Non-classical immune genes associated with pathogen recognition, such as *leucine-rich proteins* (LRPs) and *CYP450* were also among the downregulated genes. Our previous work, in which we investigated the transcriptional response of *Wolbachia*-transinfected *Ae. aegypti* mosquito cells to DENV infection showed immune-related genes such as *CYP450*, *CLIP-SP*s, and *LRPs* were predominantly upregulated [65]. *CLIP-SP*s are a diverse group of genes encoding proteolytic enzymes, and *LRP*s are associated with pathogen recognition; both play a critical role in the insects' innate immunity response such as the Toll and IMD pathways and melanization [29, 57, 94, 122, 128]. Studies in a variety of organisms, including *Ae. aegypti*, have observed enhanced expression of immune-related genes such as *AMPs*, *CLIP-SPs,* and *LRPs* in response to arbovirus infection [6, 82, 93, 141, 39, 104]. Among the commonly upregulated DEGs were genes encoding immune-related, cellular, transmembrane, transport, stress response functions, and an important virus host factor. Notably, *GNBPB4* (AAEL009178), *thioredoxin peroxidase* (*Trx*) (AAEL002309), *poor Imd response upon knock-in* (*Pirk*) (AAEL021557), *transmembrane protein 41B* (*TMEM41B*) (AAEL022930/AAEL009713), and a small number of classical and non-classical immune genes such *as CLIP-SPs*, *LRPs*, *CYP450*, *and heat shock protein 70* (*Hsp70*) were among the upregulated genes. GNBPs are Toll pathway effector defensins, and the upregulation of immune pathway-related genes, including *GNBPs*, by *Wolbachia* is consistent with other studies performed in mosquito and cell line [98, 103]. Trx are antioxidant enzymes that protect cells against reactive oxygen species (ROS) [116]. This is consistent with reports from *w*AlbB-transinfected mosquitoes, which found a number of antioxidant genes amongst the upregulated genes [98]. *Pirk* encodes a cytoplasmic protein that co-immunoprecipitates with the IMD signalling pathway and receptor peptidoglycan recognition protein LE (PGRP-LE) [59]. The IMD is primarily responsible for mounting an immune response against bacterial infection. However, overexpression of *pirk* reduced the IMD pathway response to Gram-negative bacteria in *Drosophila* and mosquitoes [59, 66, 123]. Nevertheless, these studies focused on the increased or decreased bacterial infection using Gram-negative bacteria such as *Enterobacter cloacae* and *Escherichia coli*. Notably, *Wolbachia* alters the IMD pathway directly to achieve immune tolerance and maintain its survival. A study in *w*AlbB-transinfected mosquitoes and Aag2 cell line confirmed the induction of *PGRP-LE* by *w*AlbB and supports the importance of *PGRP-LE* to *Wolbachia*'s survival within the host cell as RNAi silencing resulted in significantly decreased density [97].

TMEM41B is a pan-flavivirus host factor located in the endoplasmic reticulum (ER) membrane and was identified through a genome-wide loss of function CRISPR-Cas9 screening as a critical host factor required for flavivirus infection in mammalian and mosquito cells [43]. Effectively, TMEM41B is recruited to flavivirus RNA replication sites, mobilising lipids and inducing membrane curvature, which creates structures protecting viral RNA during replication [43, 92]. In addition to flaviviruses such as DENV, Zika virus, Yellow fever virus, and West Nile virus, this and follow-up studies in mammalian and mosquito cells found that SARS-CoV-2 of *Coronaviridae* also requires TMEM41B for infection [43, 118, 136]. Interestingly, *Wolbachia* is also located and replicates around the ER membrane of *Drosophila* and mosquito cells [30, 78, 129]. A study comparing antiviral or non-antiviral *Wolbachia* strains found that lipid droplets (LDs) increased in volume in *w*Mel- and *w*AlbB-infected cell lines and mosquito tissues compared to cells infected with *w*Pip or *Wolbachia*-free controls [78]. Remarkably, *w*Mel and *w*AlbB virus blocking strains were shown to be entirely wrapped by the host ER membrane, whereas *w*Pip was clustered separately within the host cell cytoplasm [78]. TMEM41B induction by *Wolbachia* and subsequent provision of lipids, lipid droplet formation and structural rearrangements of host ER membranes could be an undiscovered link between *Wolbachia* and its antiviral capabilities. We observed an increase of three m^6A modifications and significant upregulation of *TMEM41B* by *Wolbachia*.

In summary, we found that *Wolbachia* elevates the expression of the host's methyltransferase machinery and alters the m^6A methylation landscape in *Ae. aegypti* Aag2 mosquito cells transinfected with the *w*AlbB strain of *Wolbachia*. Interestingly, genes with reduced levels of differentially modified m^6A DRACH motifs due to *Wolbachia* are related to several functional GO terms associated with purine (adenine and guanine) nucleotide binding. The binding to adenine forms the basis for the m^6A modification to take place, and our results indicate that lower levels of m^6A DRACH motifs favour gene stability and increase the purine nucleotide binding functions critical in the post-transcriptional modification process of m^6A. Overall, we show that *Wolbachia* alters many intracellular aspects of its mosquito host by influencing post-transcriptional m^6A modifications down to gene expression, forging a symbiotic relationship while manifesting itself by encapsulating within the host's ER membrane.

Code Availability

All the algorithms and related codes used are freely available on github under open-source license agreements. Minimap2 (v.2.24): https://github.com/lh3/minimap2. SAMtools (v.1.9): https://github.com/samtools/samtools/releases/. Nanopolish (v.0.14.0): https://github.com/jts/nanopolish. xPore (v.2.1): https://github.com/GoekeLab/xpore. Bambu (v.3.2.4): https://github.com/GoekeLab/bambu. DESeq2 (v. 1.40.1): https://www.bioconductor.org/packages/release/bioc/vignettes/DESeq2/inst/doc/DESeq2.html.

Supplementary Information

The online version contains supplementary material available at https://doi.org/10.1186/s12866-025-03898-5.

Supplementary Material 1 Table S1. Primers used in this study. Table S2. Nanopore and mapping metrics. Nanopore sequencing output and QC report on raw data. Mapping to transcriptome with minimap2/v.2.24 metrics. Mapping to genome with minimap2/v.2.24 metrics. Mapping to genome with CLC Genomics Workbench 22.0. Table S3. DRACH DMR ranked. DRACH motif DMR 0.25 Positive (related to Fig. 5A). DRACH motif DMR 0.25 Negative (related to Fig. 5B). Table S4. m^6A DRACH motifs transcriptome. Table S4A. m^6A DRACH motif DMR Positive (xPore diffmod table). Table S4B. m^6A DRACH motif DMR Negative (xPore diffmod table). Table S5. DRACH motif genes. DRACH motif genes DMR Positive (620 genes). DRACH motif genes DMR Negative (506 genes). Table S6. DMR Top 20 genes. DMR Positive Top 20 genes (related to Fig. 6C). DMR Negative Top 20 genes (related to Fig. 6D). Table S7. m^6A genomic locations. Table S7A. m^6A genomic locations DMR Positive (related to Fig. 7). Table S7B. m^6A genomic locations DMR Negative (related to Fig. 7). Table S8. m^6A GO Terms. Table S8A. m^6A GO Term DMR Positive (related to Fig. 8A). Table S8B. m^6A GO Term DMR Negative (related to Fig. 8B). Table S9. DEG GO Terms. Table S9A. DEGs DESeq2 810 Protein coding genes (related to Fig. 9A). Table S9B. DESeq2 174 ncRNA (related to Fig. 9B). Table S9C. DEGs CLC-GWB 802 Protein coding genes (related to Fig. 9A). Table S9D. DESeq2 182 ncRNA (related to Fig. 9B). Table S9E. Common DEGs 643 PC between DESeq2 and CLC-GWB (related to Fig. 9C). Table S10. Chi-Square test. Table S10A. Chi-Square DMR Positive (related to Fig. 6E). Table S10B. Chi-Square DMR Negative (related to Fig. 6E). Table S10C. Chi-Square test results (related to Fig. 6E). Table S11. DEG GO Terms. Table S11A. DEG GO Terms Downregulated genes (related to Fig. 10A). Table S11B. DEG GO Terms Upregulated genes (related to Fig. 10B).

Supplementary Material 2: Fig. S1: Determination of Wolbachia density. Before Nanopore sequencing, Wolbachia density was determined by qPCR using DNA extracted from Aag2.wAlbB cells and uninfected Aag2 cells as control using primers to the wsp gene. Fig. S2. Nanopore downstream analysis workflow. Fig. S3. Principal Component analysis of the nanopore sequencing data analysed by (A) DESeq2 and (B) CLC-GWB.

Author contributions

SA conceptualized and acquired funding. ML carried out all the experiments. ML, VM, and VE analysed the data, with major contributions from ML. ML wrote the first draft. All authors contributed to editing the manuscript.

Data availability

Nanopore direct RNA sequencing data is available from The Sequence Read Archive (SRA) Bioproject accession PRJNA1169926.

Declarations

Ethics approval and consent to participate

Not applicable.

Consent for publication

Not applicable.

Competing interests

The authors declare no competing interests.

Received: 10 October 2024 / Accepted: 17 March 2025
Published online: 25 March 2025

References

1. Ahmad NA, Mancini M-V, Ant TH, Martinez J, Kamarul GMR, Nazni WA, Hoffmann AA, Sinkins SP. *Wolbachia* strain *w*AlbB maintains high density and dengue Inhibition following introduction into a field population of *Aedes aegypti*. Philos Trans R Soc B Biol Sci. 2021;376:20190809. https://doi.org/10.1098/rstb.2019.0809.
2. Alarcón CR, Lee H, Goodarzi H, Halberg N, Tavazoie SF. N^6-methyladenosine marks primary MicroRNAs for processing. Nature. 2015;519:482–5. https://doi.org/10.1038/nature14281.
3. Al-Shahrour F, Díaz-Uriarte R, Dopazo J. FatiGO: a web tool for finding significant associations of gene ontology terms with groups of genes. Bioinformatics. 2004;20:578–80. https://doi.org/10.1093/bioinformatics/btg455.
4. Amuzu HE, McGraw EA. *Wolbachia*-based dengue virus Inhibition is not tissue-specific in *Aedes aegypti*. PLoS Negl Trop Dis. 2016;10:e0005145. https://doi.org/10.1371/journal.pntd.0005145.
5. Andersen-Nissen E, Smith KD, Strobe KL, Barrett SLR, Cookson BT, Logan SM, Aderem A. Evasion of Toll-like receptor 5 by flagellated bacteria. Proc Natl Acad Sci. 2005;102:9247–52. https://doi.org/10.1073/pnas.0502040102.
6. Angleró-Rodríguez YI, MacLeod HJ, Kang S, Carlson JS, Jupatanakul N, Dimopoulos G. *Aedes aegypti* molecular responses to Zika virus: modulation of infection by the toll and Jak/Stat immune pathways and virus host factors. Front Microbiol. 2017;8:2050. https://doi.org/10.3389/fmicb.2017.02050
7. Ant TH, Herd CS, Geoghegan V, Hoffmann AA, Sinkins SP. The *Wolbachia* strain *w*Au provides highly efficient virus transmission blocking in *Aedes aegypti*. PLoS Pathog. 2018;14:e1006815. https://doi.org/10.1371/journal.ppat.1006815.
8. Arguello AE, DeLiberto AN, Kleiner RE. RNA chemical proteomics reveals the N^6-methyladenosine (m^6A)-regulated protein–RNA interactome. J Am Chem Soc. 2017;139:17249–52. https://doi.org/10.1021/jacs.7b09213.
9. Asad S, Parry R, Asgari S. Upregulation of *Aedes aegypti* Vago1 by *Wolbachia* and its effect on dengue virus replication. Insect Biochem Mol Biol. 2018;92:45–52. https://doi.org/10.1016/j.ibmb.2017.11.008.
10. Axford JK, Ross PA, Yeap HL, Callahan AG, Hoffmann AA. Fitness of *w*AlbB *Wolbachia* infection in *Aedes aegypti*: parameter estimates in an outcrossed background and potential for population invasion. Am Soc Trop Med Hyg. 2016;94:507–16. https://doi.org/10.4269/ajtmh.15-0608.
11. Bhattacharya T, Newton ILG, Hardy RW. Viral RNA is a target for *Wolbachia*-mediated pathogen blocking. PLoS Pathog. 2020;16:e1008513. https://doi.org/10.1371/journal.ppat.1008513.
12. Bhattacharya T, Newton ILG, Hardy RW. *Wolbachia* elevates host methyltransferase expression to block an RNA virus early during infection. PLoS Pathog. 2017;13:e1006427. https://doi.org/10.1371/journal.ppat.1006427.
13. Bhattacharya T, Rice DW, Crawford JM, Hardy RW, Newton ILG. Evidence of adaptive evolution in *Wolbachia*-regulated gene DNMT2 and its role in the dipteran immune response and pathogen blocking. Viruses. 2021;13:1464. https://doi.org/10.3390/v13081464.
14. Bhattacharya T, Yan L, Crawford JM, Zaher H, Newton ILG, Hardy RW. Differential viral RNA methylation contributes to pathogen blocking in *Wolbachia*-colonized arthropods. PLoS Pathog. 2022;18:e1010393. https://doi.org/10.1371/journal.ppat.1010393.
15. Bian G, Xu Y, Lu P, Xie Y, Xi Z. The endosymbiotic bacterium *Wolbachia* induces resistance to dengue virus in *Aedes aegypti*. PLoS Pathog. 2010;6:e1000833. https://doi.org/10.1371/journal.ppat.1000833.
16. Bishop C, Parry R, Asgari S. Effect of *Wolbachia w*AlbB on a positive-sense RNA negev-like virus: a novel virus persistently infecting *Aedes albopictus* mosquitoes and cells. J Gen Virol. 2020;101:216–25. https://doi.org/10.1099/jgv.0.001361.
17. Boccaletto P, Stefaniak F, Ray A, Cappannini A, Mukherjee S, Purta E, Kurkowska M, Shirvanizadeh N, Destefanis E, Groza P, Avşar G, Romitelli A, Pir P, Dassi E, Conticello SG, Aguilo F, Bujnicki JM. MODOMICS: a database of RNA

modification pathways. 2021 update. Nucleic Acids Res. 2022;50:D231–5. https://doi.org/10.1093/nar/gkab1083.
18. Boo SH, Kim YK. The emerging role of RNA modifications in the regulation of mRNA stability. Exp Mol Med. 2020;52:400–8. https://doi.org/10.1038/s12276-020-0407-z.
19. Caragata EP, Rancès E, O'Neill SL, McGraw EA. Competition for amino acids between *Wolbachia* and the mosquito host, *Aedes aegypti*. Microb Ecol. 2014;67:205–18. https://doi.org/10.1007/s00248-013-0339-4.
20. Chen Y, Sim A, Wan YK, Yeo K, Lee JJX, Ling MH, Love MI, Göke J. Context-aware transcript quantification from long-read RNA-seq data with Bambu. Nat Methods. 2023. https://doi.org/10.1038/s41592-023-01908-w.
21. Chouin-Carneiro T, Ant TH, Herd C, Louis F, Failloux AB, Sinkins SP. *Wolbachia* strain *w*AlbA blocks Zika virus transmission in *Aedes aegypti*. Med Vet Entomol. 2020;34:116–9. https://doi.org/10.1111/mve.12384.
22. Chrostek E, Marialva MSP, Yamada R, O'Neill SL, Teixeira L. High anti-viral protection without immune upregulation after interspecies *Wolbachia* transfer. PLoS ONE. 2014;9:e99025. https://doi.org/10.1371/journal.pone.0099025.
23. Csepany T, Lin A, Baldick CJ, Beemon K. Sequence specificity of mRNA N^6-adenosine methyltransferase. J Biol Chem. 1990;265:20117–22. https://doi.org/10.1016/S0021-9258(17)30477-5.
24. Cui L, Ma R, Cai J, Guo C, Chen Z, Yao L, Wang Y, Fan R, Wang X, Shi Y. RNA modifications: importance in immune cell biology and related diseases. Signal Transduct Target Ther. 2022;7:334. https://doi.org/10.1038/s41392-022-01175-9.
25. Dai Z, Asgari S. ALKBH8 as a potential N^6-methyladenosine (m^6A) eraser in insects. Insect Mol Biol. 2023;32:461–8. https://doi.org/10.1111/imb.12843.
26. Dai Z, Etebari K, Asgari S. N^6-methyladenosine modification of the *Aedes aegypti* transcriptome and its alteration upon dengue virus infection in Aag2 cell line. Commun Biol. 2022;5:607. https://doi.org/10.1038/s42003-022-03566-8.
27. Danecek P, Bonfield JK, Liddle J, Marshall J, Ohan V, Pollard MO, Whitwham A, Keane T, McCarthy SA, Davies RM, Li H. 2021. Twelve years of SAMtools and BCFtools. GigaScience 10, giab008. https://doi.org/10.1093/gigascience/giab008
28. Drazic A, Myklebust LM, Ree R, Arnesen T. The world of protein acetylation. Biochim Biophys Acta BBA - Proteins Proteom. 2016;1864:1372–401. https://doi.org/10.1016/j.bbapap.2016.06.007.
29. El Moussawi L, Nakhleh J, Kamareddine L, Osta MA. The mosquito melanization response requires hierarchical activation of non-catalytic clip domain Serine protease homologs. PLoS Pathog. 2019;15:e1008194. https://doi.org/10.1371/journal.ppat.1008194.
30. Fattouh N, Cazevieille C, Landmann F. *Wolbachia* endosymbionts subvert the Endoplasmic reticulum to acquire host membranes without triggering ER stress. PLoS Negl Trop Dis. 2019;13:e0007218. https://doi.org/10.1371/journal.pntd.0007218.
31. Ford SA, Allen SL, Ohm JR, Sigle LT, Sebastian A, Albert I, Chenoweth SF, McGraw EA. Selection on *Aedes aegypti* alters *Wolbachia*-mediated dengue virus blocking and fitness. Nat Microbiol. 2019;4:1832–9. https://doi.org/10.1038/s41564-019-0533-3.
32. Fraser JE, O'Donnell TB, Duyvestyn JM, O'Neill SL, Simmons CP, Flores HA. Novel phenotype of *Wolbachia* strain *w*Pip in *Aedes aegypti* challenges assumptions on mechanisms of *Wolbachia*-mediated dengue virus Inhibition. PLoS Pathog. 2020;16:e1008410. https://doi.org/10.1371/journal.ppat.1008410.
33. Fu Y, Dominissini D, Rechavi G, He C. Gene expression regulation mediated through reversible m^6A RNA methylation. Nat Rev Genet. 2014;15:293–306. https://doi.org/10.1038/nrg3724.
34. Geoghegan V, Stainton K, Rainey SM, Ant TH, Dowle AA, Larson T, Hester S, Charles PD, Thomas B, Sinkins SP. Perturbed cholesterol and vesicular trafficking associated with dengue blocking in *Wolbachia*-infected *Aedes aegypti* cells. Nat Commun. 2017;8:526. https://doi.org/10.1038/s41467-017-00610-8.
35. Gokhale NS, McIntyre ABR, Mattocks MD, Holley CL, Lazear HM, Mason CE, Horner SM. Altered m^6A modification of specific cellular transcripts affects *Flaviviridae* infection. Mol Cell. 2020;77:542–e5558. https://doi.org/10.1016/j.molcel.2019.11.007.
36. Gokhale NS, McIntyre ABR, McFadden MJ, Roder AE, Kennedy EM, Gandara JA, Hopcraft SE, Quicke KM, Vazquez C, Willer J, Ilkayeva OR, Law BA, Holley CL, Garcia-Blanco MA, Evans MJ, Suthar MS, Bradrick SS, Mason CE, Horner SM. N^6-methyladenosine in *Flaviviridae* viral RNA genomes regulates infection. Cell Host Microbe. 2016;20:654–65. https://doi.org/10.1016/j.chom.2016.09.015.
37. Gonzales-van Horn SR, Sarnow P. Making the mark: the role of adenosine modifications in the life cycle of RNA viruses. Cell Host Microbe. 2017;21:661–9. https://doi.org/10.1016/j.chom.2017.05.008.
38. Götz S, Garcia-Gomez JM, Terol J, Williams TD, Nagaraj SH, Nueda MJ, Robles M, Talon M, Dopazo J, Conesa A. High-throughput functional annotation and data mining with the Blast2GO suite. Nucleic Acids Res. 2008;36:3420–35. https://doi.org/10.1093/nar/gkn176.
39. Hao H, Hao S, Chen H, Chen Z, Zhang Y, Wang J, Wang H, Zhang B, Qiu J, Deng F, Guan W. *N*6-methyladenosine modification and METTL3 modulate enterovirus 71 replication. Nucleic Acids Res. 2019;47:362–74. https://doi.org/10.1093/nar/gky1007.
40. Haqshenas G, Terradas G, Paradkar PN, Duchemin J-B, McGraw EA, Doerig C. A role for the insulin receptor in the suppression of dengue virus and Zika virus in *Wolbachia*-infected mosquito cells. Cell Rep. 2019;26:529–e5353. https://doi.org/10.1016/j.celrep.2018.12.068.
41. Hendra C, Pratanwanich PN, Wan YK, Goh WSS, Thiery A, Göke J. Detection of m^6A from direct RNA sequencing using a multiple instance learning framework. Nat Methods. 2022. https://doi.org/10.1038/s41592-022-01666-1.
42. Hoffmann AA, Montgomery BL, Popovici J, Iturbe-Ormaetxe I, Johnson PH, Muzzi F, Greenfield M, Durkan M, Leong YS, Dong Y, Cook H, Axford J, Callahan AG, Kenny N, Omodei C, McGraw EA, Ryan PA, Ritchie SA, Turelli M, O'Neill SL. Successful establishment of *Wolbachia* in *Aedes* populations to suppress dengue transmission. Nature. 2011;476:454–7. https://doi.org/10.1038/nature10356.
43. Hoffmann H-H, Schneider WM, Rozen-Gagnon K, Miles LA, Schuster F, Razooky B, Jacobson E, Wu X, Yi S, Rudin CM, MacDonald MR, McMullan LK, Poirier JT, Rice CM. TMEM41B is a pan-flavivirus host factor. Cell. 2021;184:133–e14820. https://doi.org/10.1016/j.cell.2020.12.005.
44. Huang H, Weng H, Sun W, Qin X, Shi H, Wu H, Zhao BS, Mesquita A, Liu C, Yuan CL, Hu Y-C, Hüttelmaier S, Skibbe JR, Su R, Deng X, Dong L, Sun M, Li C, Nachtergaele S, Wang Y, Hu C, Ferchen K, Greis KD, Jiang X, Wei M, Qu L, Guan J-L, He C, Yang J, Chen J. Recognition of RNA N^6-methyladenosine by IGF2BP proteins enhances mRNA stability and translation. Nat Cell Biol. 2018;20:285–95. https://doi.org/10.1038/s41556-018-0045-z.
45. Huang H, Weng H, Zhou K, Wu T, Zhao BS, Sun, Mingli, Chen Z, Deng X, Xiao G, Auer F, Klemm L, Wu H, Zuo Z, Qin X, Dong Y, Zhou Y, Qin H, Tao S, Du J, Liu J, Lu Z, Yin H, Mesquita A, Yuan CL, Hu Y-C, Sun W, Su R, Dong L, Shen C, Li C, Qing Y, Jiang X, Wu X, Sun, Miao, Guan J-L, Qu L, Wei M, Müschen M, Huang G, He C, Yang J, Chen J. Histone H3 trimethylation at lysine 36 guides m^6A RNA modification co-transcriptionally. Nature. 2019;567:414–9. https://doi.org/10.1038/s41586-019-1016-7.
46. Hussain M, Frentiu FD, Moreira LA, O'Neill SL, Asgari S. *Wolbachia* uses host MicroRNAs to manipulate host gene expression and facilitate colonization of the dengue vector *Aedes aegypti*. Proc Natl Acad Sci. 2011;108:9250–5. https://doi.org/10.1073/pnas.1105469108
47. Hussain M, Zhang G, Leitner M, Hedges LM, Asgari S. *Wolbachia* RNase HI contributes to virus blocking in the mosquito *Aedes aegypti*. iScience. 2023;26:105836. https://doi.org/10.1016/j.isci.2022.105836
48. Imam H, Kim G-W, Siddiqui A. Epitranscriptomic (N^6-methyladenosine) modification of viral RNA and virus-host interactions. Front Cell Infect Microbiol. 2020;10:584283. https://doi.org/10.3389/fcimb.2020.584283.
49. Indriani C, Tantowijoyo W, Rancès E, Andari B, Prabowo E, Yusdi D, Ansari MR, Wardana DS, Supriyati E, Nurhayati I, Ernesia I, Setyawan S, Fitriana I, Arguni E, Amelia Y, Ahmad RA, Jewell NP, Dufault SM, Ryan PA, Green BR, McAdam TF, O'Neill SL, Tanamas SK, Simmons CP, Anders KL, Utarini A. Reduced dengue incidence following deployments of *Wolbachia*-infected *Aedes aegypti* in Yogyakarta, Indonesia: a quasi-experimental trial using controlled interrupted time series analysis. Gates Open Res. 2020;4:50. https://doi.org/10.12688/gatesopenres.13122.1.
50. Jansen PAM, Kamsteeg M, Rodijk-Olthuis D, Van Vlijmen-Willems IMJJ, De Jongh GJ, Bergers M, Tjabringa GS, Zeeuwen PLJM, Schalkwijk J. Expression of the Vanin gene family in normal and inflamed human skin: induction by Proinflammatory cytokines. J Invest Dermatol. 2009;129:2167–74. https://doi.org/10.1038/jid.2009.67.
51. Jia G, Fu Y, Zhao X, Dai Q, Zheng G, Yang Y, Yi C, Lindahl T, Pan T, Yang Y-G, He C. N^6-methyladenosine in nuclear RNA is a major substrate of the obesity-associated FTO. Nat Chem Biol. 2011;7:885–7. https://doi.org/10.1038/nchembio.687.
52. Jiménez NE, Gerdtzen ZP, Olivera-Nappa Á, Salgado JC, Conca C. A systems biology approach for studying *Wolbachia* metabolism reveals points of interaction with its host in the context of arboviral infection. PLoS Negl Trop Dis. 2019;13:e0007678. https://doi.org/10.1371/journal.pntd.0007678.

53. Jones P, Binns D, Chang H-Y, Fraser M, Li W, McAnulla C, McWilliam H, Maslen J, Mitchell A, Nuka G, Pesseat S, Quinn AF, Sangrador-Vegas A, Scheremetjew M, Yong S-Y, Lopez R, Hunter S. InterProScan 5: genome-scale protein function classification. Bioinformatics. 2014;30:1236–40. https://doi.org/10.1093/bioinformatics/btu031.
54. Joubert DA, Walker T, Carrington LB, De Bruyne JT, Kien DHT, Hoang NLT, Chau NVV, Iturbe-Ormaetxe I, Simmons CP, O'Neill SL. Establishment of a *Wolbachia* superinfection in *Aedes aegypti* mosquitoes as a potential approach for future resistance management. PLoS Pathog. 2016;12:e1005434. https://doi.org/10.1371/journal.ppat.1005434.
55. Kambris Z, Cook PE, Phuc HK, Sinkins SP. Immune activation by life-shortening *Wolbachia* and reduced filarial competence in mosquitoes. Science. 2009;326:134–6. https://doi.org/10.1126/science.1177531.
56. Kan RL, Chen J, Sallam T. Crosstalk between epitranscriptomic and epigenetic mechanisms in gene regulation. Trends Genet. 2022;38:182–93. https://doi.org/10.1016/j.tig.2021.06.014.
57. Kanost MR, Jiang H. Clip-domain Serine proteases as immune factors in insect hemolymph. Curr Opin Insect Sci. 2015;11:47–55. https://doi.org/10.1016/j.cois.2015.09.003.
58. Ke S, Alemu EA, Mertens C, Gantman EC, Fak JJ, Mele A, Haripal B, Zucker-Scharff I, Moore MJ, Park CY, Vågbø CB, Kusśnierczyk A, Klungland A, Darnell JE, Darnell RB. A majority of m^{6}A residues are in the last exons, allowing the potential for 3′ UTR regulation. Genes Dev. 2015;29:2037–53. https://doi.org/10.1101/gad.269415.115.
59. Kleino A, Myllymäki H, Kallio J, Vanha-aho L-M, Oksanen K, Ulvila J, Hultmark D, Valanne S, Rämet M. Pirk is a negative regulator of the *Drosophila* Imd pathway. J Immunol. 2008;180:5413–22. https://doi.org/10.4049/jimmunol.180.8.5413.
60. Koh C, Allen SL, Herbert Rl, McGraw EA, Chenoweth SF. The transcriptional response of *Aedes aegypti* with variable extrinsic incubation periods for dengue virus. Genome Biol Evol. 2018;10:3141–51. https://doi.org/10.1093/gbe/evy230.
61. Kokoza V, Ahmed A, Woon Shin S, Okafor N, Zou Z, Raikhel AS. Blocking of plasmodium transmission by cooperative action of cecropin A and defensin A in transgenic *Aedes aegypti* mosquitoes. Proc Natl Acad Sci. 2010;107:8111–6. https://doi.org/10.1073/pnas.1003056107
62. Kraemer MUG, Sinka ME, Duda KA, Mylne A, Shearer FM, Brady OJ, Messina JP, Barker CM, Moore CG, Carvalho RG, Coelho GE, Van Bortel W, Hendrickx G, Schaffner F, Wint GRW, Elyazar IRF, Teng H-J, Hay SI. The global compendium of *Aedes aegypti* and *Ae. albopictus* occurrence. Sci Data. 2015;2:150035. https://doi.org/10.1038/sdata.2015.35
63. Kumar A, Srivastava P, Sirisena P, Dubey S, Kumar R, Shrinet J, Sunil S. Mosquito innate immunity. Insects. 2018;9:95. https://doi.org/10.3390/insects9030095.
64. Lasman L, Krupalnik V, Viukov S, Mor N, Aguilera-Castrejon A, Schneir D, Bayerl J, Mizrahi O, Peles S, Tawil S, Sathe S, Nachshon A, Shani T, Zerbib M, Kilimnik I, Aigner S, Shankar A, Mueller JR, Schwartz S, Stern-Ginossar N, Yeo GW, Geula S, Novershtern N, Hanna JH. Context-dependent functional compensation between Ythdf m^{6}A reader proteins. Genes Dev. 2020;34:1373–91. https://doi.org/10.1101/gad.340695.120.
65. Leitner M, Etebari K, Asgari S. Transcriptional response of *Wolbachia*-transinfected *Aedes aegypti* mosquito cells to dengue virus at early stages of infection. J Gen Virol. 2022;103. https://doi.org/10.1099/jgv.0.001694.
66. Lhocine N, Ribeiro PS, Buchon N, Wepf A, Wilson R, Tenev T, Lemaitre B, Gstaiger M, Meier P, Leulier F. PIMS modulates immune tolerance by negatively regulating *Drosophila* innate immune signaling. Cell Host Microbe. 2008;4:147–58. https://doi.org/10.1016/j.chom.2008.07.004.
67. Li H. New strategies to improve minimap2 alignment accuracy. Bioinformatics. 2021;37:4572–4. https://doi.org/10.1093/bioinformatics/btab705.
68. Li H. Minimap2: pairwise alignment for nucleotide sequences. Bioinformatics. 2018;34:3094–100. https://doi.org/10.1093/bioinformatics/bty191.
69. Li H, Handsaker B, Wysoker A, Fennell T, Ruan J, Homer N, Marth G, Abecasis G, Durbin R, 1000 Genome Project Data Processing Subgroup. The sequence alignment/map format and samtools. Bioinformatics. 2009;25:2078–9. https://doi.org/10.1093/bioinformatics/btp352.
70. Li H, Li C, Zhang Y, Jiang W, Zhang F, Tang X, Sun G, Xu S, Dong X, Shou J, Yang Y, Chen M. Comprehensive analysis of m^{6}A methylome and transcriptome by nanopore sequencing in clear cell renal carcinoma. Mol Carcinog. 2024;63:677–87. https://doi.org/10.1002/mc.23680.
71. Liu C, Cao J, Zhang H, Wu J, Yin J. Profiling of transcriptome-wide N^6-methyladenosine (m^{6}A) modifications and identifying m^{6}A associated regulation in sperm tail formation in *Anopheles sinensis*. Int J Mol Sci. 2022;23:4630. https://doi.org/10.3390/ijms23094630.
72. Liu H, Begik O, Lucas MC, Ramirez JM, Mason CE, Wiener D, Schwartz S, Mattick JS, Smith MA, Novoa EM. Accurate detection of m^{6}A RNA modifications in native RNA sequences. Nat Commun. 2019;10:4079. https://doi.org/10.1038/s41467-019-11713-9.
73. Liu J, Yue Y, Han D, Wang X, Fu Y, Zhang L, Jia G, Yu M, Lu Z, Deng X, Dai Q, Chen W, He C. A METTL3–METTL14 complex mediates mammalian nuclear RNA N^6-adenosine methylation. Nat Chem Biol. 2014;10:93–5. https://doi.org/10.1038/nchembio.1432.
74. Liu N, Dai Q, Zheng G, He C, Parisien M, Pan T. N^6-methyladenosine-dependent RNA structural switches regulate RNA–protein interactions. Nature. 2015;518:560–4. https://doi.org/10.1038/nature14234.
75. Liu N, Zhou KI, Parisien M, Dai Q, Diatchenko L, Pan T. N^6-methyladenosine alters RNA structure to regulate binding of a low-complexity protein. Nucleic Acids Res. 2017;45:6051–63. https://doi.org/10.1093/nar/gkx141.
76. Liu-Helmersson J, Brännström Å, Sewe MO, Semenza JC, Rocklöv J. Estimating past, present, and future trends in the global distribution and abundance of the arbovirus vector *Aedes aegypti* under climate change scenarios. Front Public Health. 2019;7:148. https://doi.org/10.3389/fpubh.2019.00148.
77. Loman NJ, Quick J, Simpson JT. A complete bacterial genome assembled de Novo using only nanopore sequencing data. Nat Methods. 2015;12:733–5. https://doi.org/10.1038/nmeth.3444.
78. Loterio RK, Monson EA, Templin R, De Bruyne JT, Flores HA, Mackenzie JM, Ramm G, Helbig KJ, Simmons CP, Fraser JE. Antiviral *Wolbachia* strains associate with *Aedes aegypti* Endoplasmic reticulum membranes and induce lipid droplet formation to restrict dengue virus replication. mBio. 2024;15:e02495–23. https://doi.org/10.1128/mbio.02495-23.
79. Love MI, Huber W, Anders S. Moderated Estimation of fold change and dispersion for RNA-seq data with DESeq2. Genome Biol. 2014;15:550. https://doi.org/10.1186/s13059-014-0550-8.
80. Lu P, Bian G, Pan X, Xi Z. *Wolbachia* induces density-dependent Inhibition to dengue virus in mosquito cells. PLoS Negl Trop Dis. 2012;6:e1754. https://doi.org/10.1371/journal.pntd.0001754.
81. Lu P, Sun Q, Fu P, Li K, Liang X, Xi Z. *Wolbachia* inhibits binding of dengue and Zika viruses to mosquito cells. Front Microbiol. 2020;11:1750. https://doi.org/10.3389/fmicb.2020.01750.
82. Luplertlop N, Surasombatpattana P, Patramool S, Dumas E, Wasinpiyamongkol L, Saune L, Hamel R, Bernard E, Sereno D, Thomas F, Piquemal D, Yssel H, Briant L, Missé D. Induction of a peptide with activity against a broad spectrum of pathogens in the *Aedes aegypti* salivary gland, following infection with dengue virus. PLoS Pathog. 2011;7:e1001252. https://doi.org/10.1371/journal.ppat.1001252.
83. Maciel-de-Freitas R, Sauer FG, Kliemke K, Garcia GA, Pavan MG, David MR, Schmidt-Chanasit J, Hoffmann A, Lühken R. *Wolbachia* strains *w*Mel and *w*AlbB differentially affect *Aedes aegypti* traits related to fecundity. Microbiol Spectr. 2024;12:e00128–24. https://doi.org/10.1128/spectrum.00128-24.
84. Mancini MV, Herd CS, Ant TH, Murdochy SM, Sinkins SP. *Wolbachia* strain *w*Au efficiently blocks arbovirus transmission in *Aedes albopictus*. PLoS Negl Trop Dis. 2020;14:e0007926. https://doi.org/10.1371/journal.pntd.0007926.
85. Martinez J, Longdon B, Bauer S, Chan Y-S, Miller WJ, Bourtzis K, Teixeira L, Jiggins FM. Symbionts commonly provide broad spectrum resistance to viruses in insects: a comparative analysis of *Wolbachia* strains. PLoS Pathog. 2014;10:e1004369. https://doi.org/10.1371/journal.ppat.1004369.
86. Martinez J, Tolosana I, Ok S, Smith S, Snoeck K, Day JP, Jiggins FM. Symbiont strain is the main determinant of variation in *Wolbachia* -mediated protection against viruses across *Drosophila* species. Mol Ecol. 2017;26:4072–84. https://doi.org/10.1111/mec.14164.
87. McMeniman CJ, Lane RV, Cass BN, Fong AWC, Sidhu M, Wang Y-F, O'Neill SL. Stable introduction of a life-shortening *Wolbachia* infection into the mosquito *Aedes aegypti*. Science. 2009;323:141–4. https://doi.org/10.1126/science.1165326.
88. McMeniman CJ, O'Neill SL. A virulent *Wolbachia* infection decreases the viability of the dengue vector *Aedes aegypti* during periods of embryonic quiescence. PLoS Negl Trop Dis. 2010;4:e748. https://doi.org/10.1371/journal.pntd.0000748.
89. Meyer KD, Saletore Y, Zumbo P, Elemento O, Mason CE, Jaffrey SR. Comprehensive analysis of mRNA methylation reveals enrichment in 3′ UTRs and near stop codons. Cell. 2012;149:1635–46. https://doi.org/10.1016/j.cell.2012.05.003.

90. Molloy JC, Sommer U, Viant MR, Sinkins SP. *Wolbachia* modulates lipid metabolism in *Aedes albopictus* mosquito cells. Appl Environ Microbiol. 2016;82:3109–20. https://doi.org/10.1128/AEM.00275-16.
91. Moreira LA, Iturbe-Ormaetxe I, Jeffery JA, Lu G, Pyke AT, Hedges LM, Rocha BC, Hall-Mendelin S, Day A, Riegler M, Hugo LE, Johnson KN, Kay BH, McGraw EA, van den Hurk AF, Ryan PA, O'Neill SL. A *Wolbachia* symbiont in *Aedes aegypti* limits infection with dengue, Chikungunya, and *Plasmodium*. Cell. 2009;139:1268–78. https://doi.org/10.1016/j.cell.2009.11.042.
92. Moretti F, Bergman P, Dodgson S, Marcellin D, Claerr I, Goodwin JM, DeJesus R, Kang Z, Antczak C, Begue D, Bonenfant D, Graff A, Genoud C, Reece-Hoyes JS, Russ C, Yang Z, Hoffman GR, Mueller M, Murphy LO, Xavier RJ, Nyfeler B. TMEM 41B is a novel regulator of autophagy and lipid mobilization. EMBO Rep. 2018;19:e45889. https://doi.org/10.15252/embr.201845889.
93. Mukherjee D, Das S, Begum F, Mal S, Ray U. The mosquito immune system and the life of dengue virus: what we know and do not know. Pathogens. 2019;8:77. https://doi.org/10.3390/pathogens8020077.
94. Ng A, Xavier RJ. Leucine-rich repeat (LRR) proteins: integrators of pattern recognition and signaling in immunity. Autophagy. 2011;7:1082–4. https://doi.org/10.4161/auto.7.9.16464.
95. Nguyen TH, Nguyen HL, Nguyen TY, Vu SN, Tran ND, Le TN, Vien QM, Bui TC, Le HT, Kutcher S, Hurst TP, Duong TTH, Jeffery JAL, Darbro JM, Kay BH, Iturbe-Ormaetxe I, Popovici J, Montgomery BL, Turley AP, Zigterman F, Cook H, Cook PE, Johnson PH, Ryan PA, Paton CJ, Ritchie SA, Simmons CP, O'Neill SL, Hoffmann AA. Field evaluation of the establishment potential of *w*MelPop *Wolbachia* in Australia and Vietnam for dengue control. Parasit Vectors. 2015;8:563. https://doi.org/10.1186/s13071-015-1174-x.
96. Pajor AM, De Oliveira CA, Song K, Huard K, Shanmugasundaram V, Erion DM. Molecular basis for Inhibition of the Na^+/citrate transporter NaCT (SLC13A5) by dicarboxylate inhibitors. Mol Pharmacol. 2016;90:755–65. https://doi.org/10.1124/mol.116.105049.
97. Pan X, Pike A, Joshi D, Bian G, McFadden MJ, Lu P, Liang X, Zhang F, Raikhel AS, Xi Z. The bacterium *Wolbachia* exploits host innate immunity to Establish a symbiotic relationship with the dengue vector mosquito *Aedes aegypti*. ISME J. 2018;12:277–88. https://doi.org/10.1038/ismej.2017.174.
98. Pan X, Zhou G, Wu J, Bian G, Lu P, Raikhel AS, Xi Z. *Wolbachia* induces reactive oxygen species (ROS)-dependent activation of the toll pathway to control dengue virus in the mosquito *Aedes aegypti*. Proc Natl Acad Sci. 2012;109:E23–31. https://doi.org/10.1073/pnas.1116932108
99. Parker JS, Mizuguchi K, Gay NJ. A family of proteins related to spätzle, the toll receptor ligand, are encoded in the *Drosophila* genome. Proteins Struct Funct Bioinforma. 2001;45:71–80. https://doi.org/10.1002/prot.1125.
100. Pfaffl MW. Relative expression software tool (REST) for group-wise comparison and statistical analysis of relative expression results in real-time PCR. Nucleic Acids Res. 2002;30:e36. https://doi.org/10.1093/nar/30.9.e36.
101. Pratanwanich PN, Yao F, Chen Y, Koh CWQ, Wan YK, Hendra C, Poon P, Goh YT, Yap PML, Chooi JY, Chng WJ, Ng SB, Thiery A, Goh WSS, Göke J. Identification of differential RNA modifications from nanopore direct RNA sequencing with xPore. Nat Biotechnol. 2021;39:1394–402. https://doi.org/10.1038/s41587-021-00949-w.
102. Rainey SM, Martinez J, McFarlane M, Juneja P, Sarkies P, Lulla A, Schnettler E, Varjak M, Merits A, Miska EA, Jiggins FM, Kohl A. *Wolbachia* blocks viral genome replication early in infection without a transcriptional response by the endosymbiont or host small RNA pathways. PLoS Pathog. 2016;12:e1005536. https://doi.org/10.1371/journal.ppat.1005536.
103. Rancès E, Ye YH, Woolfit M, McGraw EA, O'Neill SL. The relative importance of innate immune priming in *Wolbachia*-mediated dengue interference. PLoS Pathog. 2012;8:e1002548. https://doi.org/10.1371/journal.ppat.1002548.
104. Reyes JIL, Suzuki Y, Carvajal T, Muñoz MNM, Watanabe K. Intracellular interactions between arboviruses and *Wolbachia* in *Aedes aegypti*. Front Cell Infect Microbiol. 2021;11:690087. https://doi.org/10.3389/fcimb.2021.690087.
105. Ridley AW, Hereward JP, Daglish GJ, Raghu S, McCulloch GA, Walter GH. Flight of *Rhyzopertha Dominica* (Coleoptera: Bostrichidae)—a spatio-temporal analysis with pheromone trapping and population genetics. J Econ Entomol. 2016;109:2561–71. https://doi.org/10.1093/jee/tow226.
106. Ritchie SA, Townsend M, Paton CJ, Callahan AG, Hoffmann AA. Application of *w*MelPop *Wolbachia* strain to crash local populations of *Aedes aegypti*. PLoS Negl Trop Dis. 2015;9:e0003930. https://doi.org/10.1371/journal.pntd.0003930.
107. Saucereau Y, Wilson TH, Tang MCK, Moncrieffe MC, Hardwick SW, Chirgadze DY, Soares SG, Marcaida MJ, Gay NJ, Gangloff M. Structure and dynamics of toll immunoreceptor activation in the mosquito *Aedes aegypti*. Nat Commun. 2022;13:5110. https://doi.org/10.1038/s41467-022-32690-6.
108. Schuster SL, Hsieh AC. The untranslated regions of mRNAs in cancer. Trends Cancer. 2019;5:245–62. https://doi.org/10.1016/j.trecan.2019.02.011.
109. Shah K, Cao W, Ellison CE. 2019. Adenine methylation in *Drosophila* is associated with the tissue-specific expression of developmental and regulatory genes. G3 genesgenomesgenetics 9, 1893–900. https://doi.org/10.1534/g3.119.400023
110. Shi H, Wang X, Lu Z, Zhao BS, Ma H, Hsu PJ, Liu C, He C. YTHDF3 facilitates translation and decay of N^6-methyladenosine-modified RNA. Cell Res. 2017;27:315–28. https://doi.org/10.1038/cr.2017.15.
111. Shi H, Wei J, He C. Where, when, and how: context-dependent functions of RNA methylation writers, readers, and erasers. Mol Cell. 2019;74:640–50. https://doi.org/10.1016/j.molcel.2019.04.025.
112. Shin SW, Bian G, Raikhel AS. A toll receptor and a cytokine, toll5A and Spz1C, are involved in toll antifungal immune signaling in the mosquito *Aedes aegypti*. J Biol Chem. 2006;281:39388–95. https://doi.org/10.1074/jbc.M608912200.
113. Sinkins SP. *Wolbachia* and arbovirus Inhibition in mosquitoes. Future Microbiol. 2013;8:1249–56. https://doi.org/10.2217/fmb.13.95.
114. Su HP, Brugnera E, Van Criekinge W, Smits E, Hengartner M, Bogaert T, Ravichandran KS. Identification and characterization of a dimerization domain in CED-6, an adapter protein involved in engulfment of apoptotic cells. J Biol Chem. 2000;275:9542–9. https://doi.org/10.1074/jbc.275.13.9542.
115. Tan L, Guo Z, Wang X, Kim DY, Li R. Utilization of nanopore direct RNA sequencing to analyze viral RNA modifications. mSystems. 2024;9:e01163–23. https://doi.org/10.1128/msystems.01163-23.
116. Tarimo B, Law H, Tao D, Pastrana-Mena R, Kanzok S, Buza J, Dinglasan R. Paraquat-mediated oxidative stress in *Anopheles Gambiae* mosquitoes is regulated by an Endoplasmic reticulum (ER) stress response. Proteomes. 2018;6:47. https://doi.org/10.3390/proteomes6040047.
117. Terradas G, McGraw EA. *Wolbachia*-mediated virus blocking in the mosquito vector *Aedes aegypti*. Curr Opin Insect Sci. 2017;22:37–44. https://doi.org/10.1016/j.cois.2017.05.005.
118. Trimarco JD, Heaton BE, Chaparian RR, Burke KN, Binder RA, Gray GC, Smith CM, Menachery VD, Heaton NS. TMEM41B is a host factor required for the replication of diverse coronaviruses including SARS-CoV-2. PLoS Pathog. 2021;17:e1009599. https://doi.org/10.1371/journal.ppat.1009599.
119. Tushev G, Glock C, Heumüller M, Biever A, Jovanovic M, Schuman EM. Alternative 3′ UTRs modify the localization, regulatory potential, stability, and plasticity of mRNAs in neuronal compartments. Neuron. 2018;98:495–e5116. https://doi.org/10.1016/j.neuron.2018.03.030.
120. Verstraete K, Verschueren KHG, Dansercoer A, Savvides SN. Acetyl-CoA is produced by the citrate synthase homology module of ATP-citrate lyase. Nat Struct Mol Biol. 2021;28:636–8. https://doi.org/10.1038/s41594-021-00624-3.
121. Vilcinskas A. Evolutionary plasticity of insect immunity. J Insect Physiol. 2013;59:123–9. https://doi.org/10.1016/j.jinsphys.2012.08.018.
122. Wang H-C, Wang Q-H, Bhowmick B, Li Y-X, Han Q. Functional characterization of two clip domain Serine proteases in innate immune responses of *Aedes aegypti*. Parasit Vectors. 2021;14:584. https://doi.org/10.1186/s13071-021-05091-9.
123. Wang M, Wang Y, Chang M, Wang X, Shi Z, Raikhel AS, Zou Z. Ecdysone signaling mediates the trade-off between immunity and reproduction via suppression of amyloids in the mosquito *Aedes aegypti*. PLoS Pathog. 2022;18:e1010837. https://doi.org/10.1371/journal.ppat.1010837.
124. Wang S, Lv W, Li T, Zhang S, Wang H, Li X, Wang L, Ma D, Zang Y, Shen J, Xu Y, Wei W. Dynamic regulation and functions of mRNA m^6A modification. Cancer Cell Int. 2022;22:48. https://doi.org/10.1186/s12935-022-02452-x.
125. Wang X, Feng J, Xue Y, Guan Z, Zhang D, Liu Z, Gong Z, Wang Q, Huang J, Tang C, Zou T, Yin P. Structural basis of N^6-adenosine methylation by the METTL3–METTL14 complex. Nature. 2016;534:575–8. https://doi.org/10.1038/nature18298.
126. Wang X, Zhao BS, Roundtree IA, Lu Z, Han D, Ma H, Weng X, Chen K, Shi H, He C. N^6-methyladenosine modulates messenger RNA translation efficiency. Cell. 2015;161:1388–99. https://doi.org/10.1016/j.cell.2015.05.014.
127. Waterhouse RM, Kriventseva EV, Meister S, Xi Z, Alvarez KS, Bartholomay LC, Barillas-Mury C, Bian G, Blandin S, Christensen BM, Dong Y, Jiang H, Kanost MR, Koutsos AC, Levashina EA, Li J, Ligoxygakis P, MacCallum RM, Mayhew GF, Mendes A, Michel K, Osta MA, Paskewitz S, Shin SW, Vlachou D, Wang L, Wei W, Zheng L, Zou Z, Severson DW, Raikhel AS, Kafatos FC, Dimopoulos G, Zdobnov EM, Christophides GK. Evolutionary dynamics of immune-related genes and pathways in disease-vector mosquitoes. Science. 2007;316:1738–43. https://doi.org/10.1126/science.1139862.

128. Waterhouse RM, Povelones M, Christophides GK. Sequence-structure-function relations of the mosquito leucine-rich repeat immune proteins. BMC Genomics. 2010;11:531. https://doi.org/10.1186/1471-2164-11-531.
129. White PM, Serbus LR, Debec A, Codina A, Bray W, Guichet A, Lokey RS, Sullivan W. Reliance of *Wolbachia* on high rates of host proteolysis revealed by a genome-wide RNAi screen of *Drosophila* cells. Genetics. 2017;205:1473–88. https://doi.org/10.1534/genetics.116.198903.
130. Willmes DM, Kurzbach A, Henke C, Schumann T, Zahn G, Heifetz A, Jordan J, Helfand SL, Birkenfeld AL. The longevity gene INDY (I'm not dead Yet) in metabolic control: potential as Pharmacological target. Pharmacol Ther. 2018;185:1–11. https://doi.org/10.1016/j.pharmthera.2017.10.003.
131. Winkler R, Gillis E, Lasman L, Safra M, Geula S, Soyris C, Nachshon A, Tai-Schmiedel J, Friedman N, Le-Trilling VTK, Trilling M, Mandelboim M, Hanna JH, Schwartz S, Stern-Ginossar N. m^{6}A modification controls the innate immune response to infection by targeting type I interferons. Nat Immunol. 2019;20:173–82. https://doi.org/10.1038/s41590-018-0275-z.
132. Xia C, Tao Y, Li M, Che T, Qu J. Protein acetylation and deacetylation: an important regulatory modification in gene transcription (Review). Exp Ther Med. 2020. https://doi.org/10.3892/etm.2020.9073.
133. Xiao W, Adhikari S, Dahal U, Chen Y-S, Hao Y-J, Sun B-F, Sun H-Y, Li A, Ping X-L, Lai W-Y, Wang X, Ma H-L, Huang C-M, Yang Y, Huang N, Jiang G-B, Wang H-L, Zhou Q, Wang X-J, Zhao Y-L, Yang Y-G. Nuclear m^{6}A reader YTHDC1 regulates mRNA splicing. Mol Cell. 2016;61:507–19. https://doi.org/10.1016/j.molcel.2016.01.012.
134. Xu T, Wu X, Wong CE, Fan S, Zhang Y, Zhang S, Liang Z, Yu H, Shen L. FIONA1-mediated m^{6}A modification regulates the floral transition in *Arabidopsis*. Adv Sci. 2022;9:2103628. https://doi.org/10.1002/advs.202103628.
135. Ye J, Coulouris G, Zaretskaya I, Cutcutache I, Rozen S, Madden TL. Primer-BLAST: a tool to design target-specific primers for polymerase chain reaction. BMC Bioinformatics. 2012;13:134. https://doi.org/10.1186/1471-2105-13-134.
136. Yousefi M, Lee WS, Yan B, Cui L, Yong CL, Yap X, Tay KSL, Qiao W, Tan D, Nurazmi NI, Linster M, Smith GJD, Lee YH, Carette JE, Ooi EE, Chan KR, Ooi YS. TMEM41B and VMP1 modulate cellular lipid and energy metabolism for facilitating dengue virus infection. PLoS Pathog. 2022;18:e1010763. https://doi.org/10.1371/journal.ppat.1010763.
137. Zhang D, Wang Y, He K, Yang Q, Gong M, Ji M, Chen L. *Wolbachia* limits pathogen infections through induction of host innate immune responses. PLoS ONE. 2020;15:e0226736. https://doi.org/10.1371/journal.pone.0226736.
138. Zhang G, Hussain M, Asgari S. Regulation of arginine methyltransferase 3 by a *Wolbachia*-induced microRNA in *Aedes aegypti* and its effect on wolbachia and dengue virus replication. Insect Biochem Mol Biol. 2014;53:81–8. https://doi.org/10.1016/j.ibmb.2014.08.003
139. Zhang G, Hussain M, O'Neill SL, Asgari S. *Wolbachia* uses a host microRNA to regulate transcripts of a methyltransferase, contributing to dengue virus Inhibition in *Aedes aegypti*. Proc Natl Acad Sci. 2013;110:10276–81. https://doi.org/10.1073/pnas.1303603110
140. Zhang Y, Geng X, Li Q, Xu J, Tan Y, Xiao M, Song J, Liu F, Fang C, Wang H. m^{6}A modification in RNA: biogenesis, functions and roles in gliomas. J Exp Clin Cancer Res. 2020;39:192. https://doi.org/10.1186/s13046-020-01706-8.
141. Zhao L, Alto B, Shin D. Transcriptional profile of *Aedes aegypti* leucine-rich repeat proteins in response to Zika and Chikungunya viruses. Int J Mol Sci. 2019;20:615. https://doi.org/10.3390/ijms20030615.
142. Zheng G, Dahl JA, Niu Y, Fedorcsak P, Huang C-M, Li CJ, Vågbø CB, Shi Y, Wang W-L, Song S-H, Lu Z, Bosmans RPG, Dai Q, Hao Y-J, Yang X, Zhao W-M, Tong W-M, Wang X-J, Bogdan F, Furu K, Fu Y, Jia G, Zhao X, Liu J, Krokan HE, Klungland A, Yang Y-G, He C. ALKBH5 is a mammalian RNA demethylase that impacts RNA metabolism and mouse fertility. Mol Cell. 2013;49:18–29. https://doi.org/10.1016/j.molcel.2012.10.015.
143. Zhou J, Wan J, Gao X, Zhang X, Jaffrey SR, Qian S-B. Dynamic m^{6}A mRNA methylation directs translational control of heat shock response. Nature. 2015;526:591–4. https://doi.org/10.1038/nature15377.
144. Zhou Y, Ćorović M, Hoch-Kraft P, Meiser N, Mesitov M, Körtel N, Back H, Naarmann-de Vries IS, Katti K, Obrdlík A, Busch A, Dieterich C, Vaňáčová Š, Hengesbach M, Zarnack K, König J. m^{6}A sites in the coding region trigger translation-dependent mRNA decay. Mol Cell. 2024;84:4576–e459312. https://doi.org/10.1016/j.molcel.2024.10.033.

Publisher's note